

7 (12)

DNA 4245T

ADA 043571

PLASMA PHYSICS MECHANISMS RELEVANT TO STRIATION STRUCTURING AND DECAY

Part 1 - Aspects of Striation Decay

Part 2 - A Synopsis of Drift Mode Behavior

Part 3 - Velocity Shear, the $E \times B$ Instability and the k^{-2} Power Density Spectrum

JAYCOR
1401 Camino Del Mar
Del Mar, California 92014

1 February 1977

Final Report for Period 22 December 1975—21 December 1976

CONTRACT No. DNA 001-76-C-0186

APPROVED FOR PUBLIC RELEASE;
DISTRIBUTION UNLIMITED.

THIS WORK SPONSORED BY THE DEFENSE NUCLEAR AGENCY
UNDER RDT&E RMSS CODE B322076464 S99QAXHC04107 H2590D.

DDC FILE COPY

Prepared for
Director
DEFENSE NUCLEAR AGENCY
Washington, D. C. 20305

DDC
RECEIVED
AUG 31 1977
RECEIVED
B
LET

Destroy this report when it is no longer
needed. Do not return to sender.



9 Final rept. 22 Dec 75-21 Dec 76

UNCLASSIFIED

SECURITY CLASSIFICATION OF THIS PAGE (When Data Entered)

REPORT DOCUMENTATION PAGE		READ INSTRUCTIONS BEFORE COMPLETING FORM
1. REPORT NUMBER DNA 4245T 19 ✓	2. GOVT ACCESSION NO.	3. RECIPIENT'S CATALOG NUMBER
4. TITLE (and Subtitle) PLASMA PHYSICS MECHANISMS RELEVANT TO STRIATION STRUCTURING AND DECAY. Part 1—Aspects of Striation Decay. Part 2—A Synopsis of Drift Mode Behavior.	5. TYPE OF REPORT & PERIOD COVERED Topical Report for Period 22 Dec 75—21 Dec 76	
7. AUTHOR(s) S. Robert/Goldman	14. PERFORMING ORG. REPORT NUMBER 177-75014-FR	15. CONTRACT OR GRANT NUMBER(s) DNA 001-76-C-0186 new
9. PERFORMING ORGANIZATION NAME AND ADDRESS JAYCOR 1401 Camino Del Mar Del Mar, California 92014	10. PROGRAM ELEMENT PROJECT, TASK AREA & WORK UNIT NUMBERS Subtask S99QAXHC041-07	
11. CONTROLLING OFFICE NAME AND ADDRESS Director Defense Nuclear Agency Washington, D.C. 20305	12. REPORT DATE 1 Feb 1977 ✓	13. NUMBER OF PAGES 86 12820
14. MONITORING AGENCY NAME & ADDRESS (if different from Controlling Office)	15. SECURITY CLASS (of this report) UNCLASSIFIED	
16. DISTRIBUTION STATEMENT (of this Report) Approved for public release; distribution unlimited.		
17. DISTRIBUTION STATEMENT (of the abstract entered in Block 20, if different from Report)		
18. SUPPLEMENTARY NOTES This work sponsored by the Defense Nuclear Agency under RDT&E RMSS Code B322076464 S99QAXHC04107 H2590D.		
19. KEY WORDS (Continue on reverse side if necessary and identify by block number)		
20. ABSTRACT (Continue on reverse side if necessary and identify by block number) Part 1—We have surveyed aspects of striation decay due to both ionization falling (and the subsequent recombination) and diffusion perpendi- cular to the magnetic field. Among the phenomena assessed are: 1. Ionized material falling due to motion parallel to the magnetic field, B, which is allowed to make an arbitrary angle with the vertical.		

3922207B

UNCLASSIFIED

SECURITY CLASSIFICATION OF THIS PAGE (When Data Entered)

4. TITLE (and Subtitle) (Continued)

Part 3—Velocity Shear, the $E \times B$ Instability and the k^{-2} Power Density Spectrum.

20. ABSTRACT (Continued)

2. Striation falling due to motion perpendicular to \vec{B} . (This occurs for a nonvertical magnetic field through the setting up of electric fields perpendicular to \vec{B} due to components of the neutral velocity or gravity perpendicular to \vec{B} .)
3. Diffusion perpendicular to \vec{B} due to drift-dissipation mode turbulence.
4. Distance scales for striation structure for model situations of striation pinching and striation tip steepening. (The scales are calculated as functions of initial dimensions and diffusion coefficients.
5. Time scales for striation decay due to the above processes.

The effect of ionization falling appears to be capable of removing striation inhomogeneities on a time scale of order 1 hour; diffusion perpendicular to the magnetic field is strongly dependent on striation dimensions and diffusion mechanisms, but significant turbulent diffusion appears possible in some cases on time scales of the order of ten minutes. There is some indication in the experimental data of plasma turbulent diffusion. These results are of the nature of estimates rather than detailed calculations and hence are suggestive rather than definitive.

Part 2—In this paper we have attempted to present a basis for the physical understanding of drift modes as well as background information for their application to striation decay problems. If one neglects the effect of a component of the ambient electric field, E , in the direction of the background density gradient, ∇n (with both perpendicular to the ambient magnetic field, B), drift modes appear capable of preventing elongated striations from getting thinner than 0.1 km in many cases of interest. The inclusion of electric field effects for drift modes is an ongoing problem.

Part 3—The $E \times B$ instability is analyzed in the presence of plasma velocity shear, with the magnetic field, B , in the z -direction, the background density gradient in the x -direction, and electric field components E_x and E_y with E_x/E_y non-zero. It is shown that the structure of $E \times B$ modes under these circumstances can account naturally for a k^{-2} ionospheric power density spectrum, provided one assumes that the modes grow until the modal density gradient in the direction of the ambient density gradient becomes comparable with the ambient density gradient.

UNCLASSIFIED

SECURITY CLASSIFICATION OF THIS PAGE (When Data Entered)

SUMMARY

JAYCOR work on striation decay during the past year is summarized in the three accompanying reports, "Aspects of Striation Decay," "A Synopsis of Drift Mode Behavior," and "Velocity Shear, the $E \times B$ Instability and the k^{-2} Power Density Spectrum."

The first report presents estimates that plasma striations could decay due to ionization falling (and the resultant recombination) on the time scale of an hour and due to plasma turbulence from drift-dissipative modes on time scales of the order of ten minutes (under appropriate ambient conditions); further the competition between ordinary collisional diffusion and drift-dissipative diffusion is assessed and conditions for dominance of the turbulent effects (sometimes by a factor of 100) are established; in addition models are introduced to study the effect of sensitivity of striation decay time to variable diffusion coefficient. Finally it is established that 0.1-0.2 km structures associated with anomalous gigahertz scintillation can be explained by a balance between drift-dissipative diffusion and convection whereas they cannot be explained by a balance between collisional diffusion and convection. Hence we consider that the first report serves as a justification for the relevance of plasma turbulence behavior to striation decay. The use of drift-dissipative turbulence is to some extent illustrative and tends to establish a lower bound for turbulent effects.

The second report is an introduction to drift wave phenomenology with relevance to the striation decay problem. It is meant to indicate how properties of drift modes used in the first report were obtained as well as to indicate a physical

picture for the instability mechanism and a justification for usage of the drift-dissipative mode instead of other drift modes. It also indicates some of the caveats necessary when dealing with applications of drift waves to the striation decay problem.

The third report presents a theory for establishment of the k^{-2} power density spectrum on the basis of $E \times B$ eigenmodes with plasma velocity shear ($E =$ electric field, $n =$ ionized density, $E \cdot \nabla n \neq 0$). We feel that this study of yet another form of possible plasma turbulence is significant because of its direct connection to the experimentally observed spectrum and the resulting possibility of experimental examination, as well as its eventual application to striation decay. To our knowledge although there has been much previous work on $E \times B$ turbulence, this is the first work entirely within the scope of $E \times B$ turbulence which provides an explanation for the k^{-2} power density spectrum.

ACCESSION for	
NTIS	White Section <input checked="" type="checkbox"/>
DDC	Buff Section <input type="checkbox"/>
UNANNOUNCED	<input type="checkbox"/>
JUSTIFICATION	
BY	
DISTRIBUTION/AVAILABILITY CODES	
Dist.	AVAIL. and/or SPECIAL
A	

CONTENTS

	<u>Page</u>
Part 1 - ASPECTS OF STRIATION DECAY	1-1
1. INTRODUCTION	1-3
2. MECHANISMS AFFECTING SINKING OF IONIZATION	1-4
2.1 Vertical Contributions Due to Force Components Parallel to \vec{B}	1-4
2.2 Recombination Mechanism - Charge Exchange Followed by Dissociative Recombination	1-5
2.3 Discussion of Contributions	1-5
2.4 Additional Contributions under Disturbed Nuclear Conditions	1-5
2.5 Contributions Due to Force Components Perpendicular to \vec{B}	1-6
3. CONTRIBUTION TO STRIATION DECAY FROM DIFFUSION PERPENDICULAR TO \vec{B}	1-10
3.1 Diffusion Mechanisms	1-10
3.2 Relation Between the Size of Various Parts of the Striation, Striation Decay, and Diffusion Coefficient	1-14
4. DISCUSSION	1-19
5. FUTURE PRIORITIES	1-22
REFERENCES	1-25
APPENDIX A. CONVECTIVE MOTION PERPENDICULAR TO \vec{B} THROUGH ELECTRIC POLARIZATION	1-27
Part 2 - A SYNOPSIS OF DRIFT MODE BEHAVIOR	2-1
1. INTRODUCTION	2-3
2. BASIC MECHANISM FOR NEUTRALLY STABLE DRIFT WAVE	2-5
2.1 Characteristics of Background Plasma	2-5
2.2 Mode Structure	2-5

	<u>Page</u>
3. INSTABILITY MECHANISM FOR DRIFT WAVES	2-8
3.1 Equivalence of $\sin \Delta > 0$ and Net Flux Against Background Density Gradient	2-8
3.2 Relation Between γ and $\sin \Delta$	2-10
3.3 Equivalence of $\omega_r - kv_{De} < 0$ and $ \omega_r - kv_{De} \ll \omega_r$ with Instability.	2-10
3.4 Ion Behavior	2-11
4. RELATION TO OTHER TYPES OF DRIFT MODES	2-13
5. GROWTH RATES AND PARAMETER RANGES FOR DRIFT DISSIPATIVE MODES	2-14
6. DIFFUSION COEFFICIENT FROM DRIFT-DISSIPATIVE MODES; ADDITIONAL PHYSICAL EFFECTS	2-17
7. SUMMARY	2-20
REFERENCES	2-21
Part 3 - VELOCITY SHEAR, THE $E \times B$ INSTABILITY AND THE k^{-2} POWER DENSITY SPECTRUM	3-1
1. INTRODUCTION	3-3
2. GENERAL ANALYSIS	3-6
3. ASYMPTOTIC ANALYSIS FOR $kLE_x/E_y \gg 1$, $kL \gg 1$	3-8
4. ASYMPTOTIC ANALYSIS FOR $kLE_x/E_y \approx 1$, $kL \gg 1$	3-13
5. SUMMARY OF $E \times B$ MODES WITH BACKGROUND PLASMA VELOCITY SHEAR	3-19
6. RELEVANCE TO THE k^{-2} POWER DENSITY SPECTRUM	3-21
REFERENCES	3-25

PART 1
ASPECTS OF STRIATION DECAY

CONTENTS

	<u>Page</u>
1. INTRODUCTION	1-3
2. MECHANISMS AFFECTING SINKING OF IONIZATION	1-4
2.1 Vertical Contributions Due to Force Components Parallel to \vec{B}	1-4
2.2 Recombination Mechanism - Charge Exchange Followed by Dissociative Recombination	1-5
2.3 Discussion of Contributions	1-5
2.4 Additional Contributions under Disturbed Nuclear Conditions	1-5
2.5 Contributions Due to Force Components Perpendicular to \vec{B}	1-6
3. CONTRIBUTION TO STRIATION DECAY FROM DIFFUSION PERPENDICULAR TO \vec{B}	1-10
3.1 Diffusion Mechanisms	1-10
3.2 Relation Between the Size of Various Parts of the Striation, Striation Decay, and Diffusion Coefficient	1-14
4. DISCUSSION	1-19
5. FUTURE PRIORITIES	1-22
REFERENCES AND FOOTNOTES	1-25
APPENDIX A. CONVECTIVE MOTION PERPENDICULAR TO \vec{B} THROUGH ELECTRIC POLARIZATION	1-27

1. INTRODUCTION

 The purpose of this report is to present various factors affecting striation decay as well as to indicate their significance in terms of possible time scales for striation decay and spatial structuring of striations. In the second section mechanisms affecting sinking of ionization both parallel and perpendicular to \vec{B} are presented and time scales estimated. In the third section diffusion due to one type of plasma turbulence is presented as well as ordinary collisional diffusion. Some aspects of the interplay of diffusion with spatial structure and striation evolution are shown. These are used to assess the dependence of decay on diffusion coefficient as well as to infer the possibility of plasma turbulence diffusion in observational situations. In the fourth section our results are summarized both as to decay and spatial structuring of striations. In the fifth section, suggestions for future work are made. 

2. MECHANISMS AFFECTING SINKING OF IONIZATION

Contributions 2.1 through 2.4 refer to sinking and decay due to ionization motion parallel to \vec{B} . Contribution 2.5 refers to sinking of density enhancements due to force components perpendicular to \vec{B} .

2.1 VERTICAL CONTRIBUTIONS DUE TO FORCE COMPONENTS PARALLEL TO \vec{B}

The separate contributions in this category are labelled v_1 , v_2 and v_3 . We have:

$$a) \quad v_1 = -v_n \cos D \sin D \quad (1)$$

where

v_n = northward component of neutral wind,

D = dip angle,

v_1 is contribution from vertical component of the horizontal neutral wind projected onto an (inclined) magnetic field.

Fig. 1a illustrates v_1 .

$$b) \quad v_2 = \frac{-\sin^2 D}{n_i} \frac{k}{v_{in} m_i} \frac{\partial}{\partial z} n_i (T_e + T_i) \quad (2)$$

v_2 is contribution from diffusion parallel to B projected vertically, n_i = ion density, v_{in} = ion-neutral collision frequency, k = Boltzmann's constant, m_i = ion mass, z = vertical coordinate, T_e = electron temperature, T_i = ion temperature, z is vertical coordinate.

$$c) \quad v_3 = \frac{g \sin^2 D}{v_{in}} \quad (3)$$

v_3 is the fall from gravity, g = gravitational acceleration.

2.2 RECOMBINATION MECHANISM - CHARGE EXCHANGE FOLLOWED BY DISSOCIATIVE RECOMBINATION⁽¹⁾

The loss rate is of the form

$$- k_1 n(O_2) + k_2 n(N_2) n_i \quad (4)$$

Here k_1 and k_2 are constants, $n(O_2)$ and $n(N_2)$ are molecular oxygen and nitrogen densities.

2.3 DISCUSSION OF CONTRIBUTIONS

Gravity pulls ionized particles down the field line, at night the neutral wind pushes ionized particles up the field lines ($v_n < 0$), during the day the neutral wind pulls ionized particles down the field lines ($v_n > 0$), thermal diffusion (proportional to the ionized particle pressure gradient) can act in both directions.

The ion continuity equation is:

$$\frac{\partial n_i}{\partial t} + \frac{\partial}{\partial z} [n_i (v_1 + v_2 + v_3)] = Q - [k_1 n(O_2) + k_2 n(N_2)] n_i \quad (5)$$

where Q represents creation and z is the vertical coordinate. During days relative striation densities will be dropped down by Q as well as all other factors except thermal diffusion. At night Q is negligible, Eq. (5) is linear in n_i (neglecting entrainment of neutrals due to very high ionized densities) and decay time scales of 2 hours⁽²⁾ (e-folding in 2 hours) appears reasonable.

2.4 ADDITIONAL CONTRIBUTIONS UNDER DISTURBED NUCLEAR CONDITIONS

For disturbed situations vertical neutral winds initially upwards but eventually downwards (F. Fajen and R. W. Kilb, private communication) could play a profound role in pulling ionized particles down the field lines. Ionized material returning from the magnetosphere could perform the same function.

There could be strong effects due to disturbed neutral wind inhomogeneities.

2.5 CONTRIBUTIONS DUE TO FORCE COMPONENTS PERPENDICULAR TO \vec{B}

These can involve neutral winds, gravity and electric fields. Thermal diffusion $\perp \vec{B}$ should be insignificant compared to that $\parallel \vec{B}$. In the generally appropriate limit,

$$\frac{\nu_{en}}{\omega_{ce}} \ll \frac{\nu_{in}}{\omega_{ci}} \ll 1 ,$$

(ν_{en} = electron-neutral collision frequency, ω_{ce} = electron cyclotron frequency) electrons can only move with velocity,

$$\frac{c\mathbf{E} \times \mathbf{B}}{B^2}$$

where

$$\mathbf{E} = \mathbf{E}_{\perp 0} - \nabla_{\perp} \psi$$

(Here $\mathbf{E}_{\perp 0}$ is the spatially uniform, ambient electric field ($\perp \vec{B}$) and $-\nabla_{\perp} \psi$ is the self-consistent induced electric field $\perp \mathbf{B}$.) Hence, by quasi-neutrality of ions and electrons, the problem of determining ionization density changes $\perp \vec{B}$ is equivalent to finding ψ . We take ψ to be given by:

$$\nabla_{\perp} \cdot \left[\left(\mathbf{E}_0 + \frac{\mathbf{v} \times \mathbf{B}}{c} - \nabla_{\perp} \psi \right) \Sigma + \frac{e \vec{g} \times \mathbf{B}}{\omega_{ci} |\mathbf{B}|} N \right] = 0 \quad (6)$$

where, with \tilde{z} denoting location along a magnetic field line,

$$\Sigma = \int_0^{\infty} d\tilde{z} n_i \frac{\nu_{in} e c}{\omega_{ci} B} ,$$

$$N = \int_0^{\infty} d\tilde{z} n_i ,$$

and \vec{v} is a mean value for the field line integrated neutral wind,

$$\vec{v} \Sigma = \int_0^{\infty} \vec{v}(\tilde{z}) d\tilde{z} n_i \frac{\nu_{in} e c}{\omega_{ci} B} .$$

This equation is based on Eq. (13) of Reference 3 with the assumptions:

1. Neglect of higher order terms in v_{in}/ω_{ci} ,
2. $E_{\perp 0}$, \vec{v} and \vec{g} are constant in space (n.b., \vec{v} is a field line average).
3. On defining E_{eff} as the maximum of $|\vec{E}_0|$, $|\vec{v}|B/c$ and $|\vec{g}|N_e/(\Sigma\omega_{ci})$,

$$L_{\perp} > \frac{2T}{e E_{eff}}$$

and

$$h_n > \frac{2T}{e E_{eff}}$$

where h_n is the scale height for neutral variation.

Using a waterbag model, (4)

$$\Sigma = \Sigma_1, \quad \rho < \rho_0; \quad \Sigma = \Sigma_2, \quad \rho > \rho_0$$

$$N = N_1, \quad \rho < \rho_0; \quad N = N_2, \quad \rho > \rho_0$$

where ρ is the cylindrical radius around the axis in the direction of $\vec{B}/|B|$, we have (see Appendix A for details)

$$\begin{aligned} v_{\perp} = & \frac{cE_{\perp 0} \times B}{B^2} \frac{2\Sigma_2}{\Sigma_1 + \Sigma_2} \\ & + \frac{c}{B^2} \frac{(\Sigma_2 - \Sigma_1)}{\Sigma_1 + \Sigma_2} \left[\frac{(\vec{v} \times B) \times B}{c} + \frac{(N_1 - N_2)}{\Sigma_1 - \Sigma_2} \frac{e(\vec{g} \times B) \times B}{\omega_{ci} |B|} \right] \end{aligned} \quad (7)$$

If there is no inhomogeneity in $\Sigma_2 = \Sigma_1$, $N_1 = N_2$ and

$$v_{\perp} = \frac{c E_{\perp 0} \times B}{B^2}$$

Hence there is a vertical velocity

$$\frac{c E_{\perp 0} \cdot e_e}{B} \cos D$$

where e_e is the unit vector in the east direction. Indications in Reference 2 are that this is not a very significant effect.

For $\Sigma_1 \gg \Sigma_2$ and $N_1 \gg N_2$, the vertical component of v_{\perp} is

$$v_{\perp v} = v_n \sin I \cos I - \frac{g \cos^2 I}{\langle v_{in} \rangle} \quad (8)$$

where

$$\langle v_{in} \rangle = \int_0^{\infty} n_i v_{in} dz / \int_0^{\infty} n_i dz$$

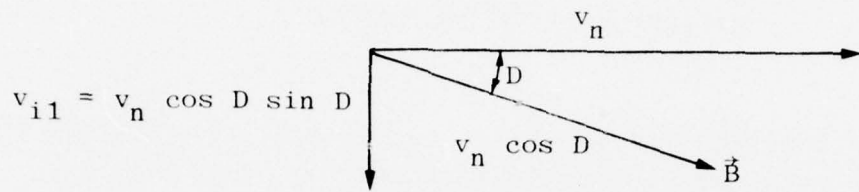
The neutral wind driven contribution to Eq. (8) is shown in Fig. 1b. It is interesting to note on combining Eqs. (1)-(3) and (8) that in this limit the cloud has a net upward velocity (neglecting altitude differences in v_{in} so that $v_{in} \approx \langle v_{in} \rangle$) of:

$$-\frac{\sin^2 I}{n_i} \frac{k}{v_{in} m_i} \frac{\partial}{\partial z} [n_i (T_e + T_i)] - \frac{g}{\langle v_{in} \rangle}$$

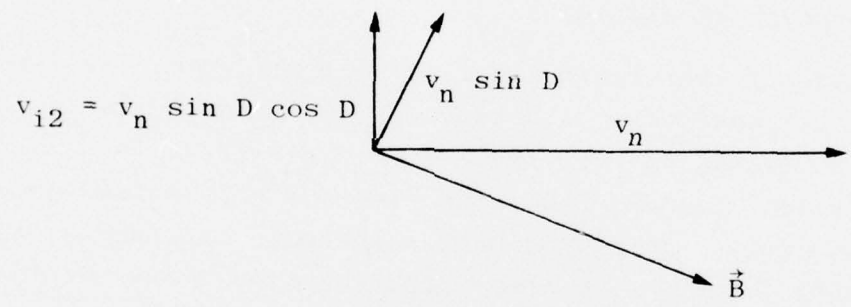
i.e., horizontal neutral winds do not lower the cloud (illustrated in Fig. 1) and gravity lowers it as if the magnetic field were nonexistent. This would characteristically result in decay time states which are at least a factor of $\sin^2 D$ lower than the spatially homogeneous decay time scale.

This limit is of course suggestive rather than fully realistic. However through Eq. (8), one sees that at night (since $v_n < 0$) the effect of finite dimensions perpendicular to \vec{B} is to increase the sinking rate of density enhancements relative to the ambient.

a) v_{i1} , due to force components $\parallel \vec{B}$; horizontal neutral wind



b) v_{i2} , due to force components $\parallel \vec{B}$ (if striation conductivity large compared to ambient); horizontal neutral wind.



Note $v_{i1} + v_{i2} = 0$.

Figure 1. Illustrative Vertical Ionized Velocity Components.

3. CONTRIBUTION TO STRIATION DECAY FROM DIFFUSION PERPENDICULAR TO \vec{B}

The contribution to striation decay from diffusion perpendicular to \vec{B} depends on two factors:

1. What are the mechanisms responsible for diffusion.
2. What is the striation geometry (shapes and dimensions) and what is the non-diffusive flow on which diffusions is superimposed.

3.1 DIFFUSION MECHANISMS

Classical ion-electron collisional diffusion for circular striations perpendicular to \vec{B} has been investigated in detail by Kilb and Stagat.⁽⁵⁾ For the electron density $n_e = n_i = 10^6 \text{ cm}^{-3}$ and a striation width of 1 km, the time for a 2.25-fold decay of density (due to a cylindrical radius increase of a factor of 1.5) is about 1 hour. For lower densities and larger striation radii decay times would be greater.

We have investigated drift-dissipative modes⁽⁶⁾ (DDM) as a source of striation diffusion. The DDM which are pictured to grow on a background provided by the striation structure (see Fig. 2) serve to diffuse the striation. Our results are based on the assumption that DDM are not sensitive to background electric fields. This appears likely but has not been theoretically verified. The fastest growing DDM are typically 20 meters in wavelength.

To understand the range of applicability of DDM, we define

$$c_s = \sqrt{\frac{k(T_e + T_i)}{m_i}}$$

and

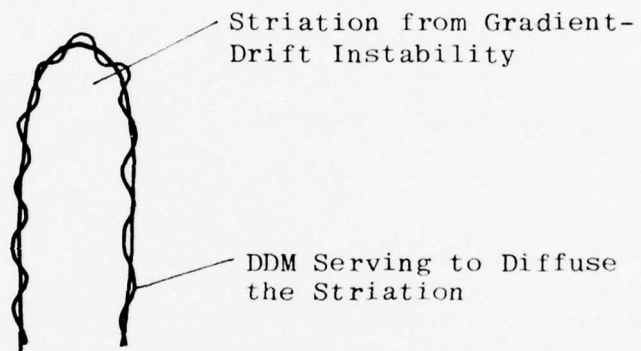


Figure 2. Geometry for DDM Diffusion.

$$\nu_i = \nu_{in} + 0.15 \frac{k_y^2 C_s^2}{\omega_{ci}} \nu_{ii} ,$$

where k_y is the DDM wave vector and ν_{ii} is the ion-ion collision frequency. Then for $L_{\perp} \gg C_s/\nu_i$ and

$$L_{\parallel} \gg 2\pi \left(\frac{C_s L_{\perp} m_i}{m_e \nu_e} \right)^{\frac{1}{2}} ,$$

where L_{\perp} is the scale length for density variation $\perp \vec{B}$, L_{\parallel} is the scale length for density variation $\parallel \vec{B}$, and $\nu_e = \nu_{en} + \nu_{ei}$, with ν_{en} the electron-neutral collision frequency and ν_{ei} the electron-ion collision frequency. Our calculations show for

$$\frac{k_y^2 C_s^2}{\omega_{ci}} = 1$$

(which we are free to choose) and

$$k_z = k_y \left(\frac{\nu_e C_s}{\omega_{ce} \omega_{ci} L_{\perp}} \right)^{\frac{1}{2}}$$

for the DDM growth rate, γ ,

$$\gamma \approx 0.07 \frac{C_s}{L_{\perp}} \text{ sec}^{-1} .$$

For the neutral density $n \leq 2.0 \times 10^8$ and $n_e \leq 10^6 \text{ cm}^{-3}$ as commonly met at night at altitudes above 400 km⁽⁷⁾ the conditions on L_{\perp} and L_{\parallel} hold for $L_{\perp} \ll 1 \text{ km}$ and $L_{\parallel} \gg 8 \text{ km}$. Here we have used,

$$\nu_e = 3.5 \times 10^{-9} n + 10^{-3} n_e ,$$

$$\nu_i = 8.3 \times 10^{-10} n + 5 \times 10^{-7} n_e ,$$

$$T_e = T_i = 0.1 \text{ eV} .$$

The resulting diffusion coefficient is⁽⁸⁾:

$$D_{\perp} = \frac{\gamma}{k_x^2} \approx 0.07 \frac{C_S}{L_{\perp}} \rho_i L_{\perp} = 0.07 \frac{C_S^2}{\omega_{ci}}$$

Here, k_x is the DDM wave-vector in the direction of density variation. Our calculations show $k_x \approx (\rho_i L_{\perp})^{-\frac{1}{2}}$ where ρ_i is an effective ion-Larmor radius equal to C_S/ω_{ci} . This results in a diffusion time estimate of

$$\frac{L_{\perp}^2}{D_{\perp}} = \frac{L_{\perp}^2 \omega_{ci}}{0.07 C_S^2}$$

For a striation width of 0.1 km, corresponding to $L_{\perp} = 5 \times 10^{-2}$ km,

$$\frac{L_{\perp}^2 \omega_{ci}}{0.07 C_S^2} = 10 \text{ seconds}$$

This corresponds to the previously mentioned electron-ion collisional diffusion time of about 1 hour.

Put another way, for diffusion due to electron-ion collisions

$$D_{\perp} = \frac{\nu_{ei}}{\omega_{ce}} \frac{c k (T_e + T_i)}{q B} = \frac{\nu_{ei}}{\omega_{ce}} \frac{C_S^2}{\omega_{ci}}$$

where ν_{ei} is the electron-ion collision frequency. Using $n_e = 10^6$, $T_i = T_e = 0.1$ eV, $B = 0.5$ gauss results in

$$D_{\perp} = 8 \times 10^3 \text{ cm}^2/\text{sec} \quad (9a)$$

This compares with the drift-dissipative estimate,

$$D_{\perp} = 0.07 \frac{C_S^2}{\omega_{ci}} = 2.5 \times 10^6 \text{ cm}^2/\text{sec} \quad (9b)$$

under the same conditions (with $n \leq 2.0 \times 10^8 \text{ cm}^{-3}$).

3.2 RELATION BETWEEN THE SIZE OF VARIOUS PARTS OF THE STRIATION, STRIATION DECAY, AND DIFFUSION COEFFICIENT

To heuristically treat the interplay between striation geometry and diffusion coefficient and to attempt to infer the presence of DDM we consider the model of an incompressible flow perpendicular to \vec{B} to which a diffusive contribution will be added. Typically striations evolve into sheet-like structures which then form "bubbles" or break up into parts. Estimates apply to two situations which appear to develop in striation evolution. These are sheet pinching-off (Fig. 3a) and striation tip steepening (Fig. 3b).

For the first situation, Fig. 3a, we consider the elongation of a density enhancement in the y-direction, due, for instance, to an ambient electric field, E_{Ox} , in the negative x-direction. We take the magnetic field in the z-direction and

$$\nabla \cdot \vec{v} = 0 \quad (10)$$

where \vec{v} is the convective, as distinct from diffusive, electron velocity perpendicular to the magnetic field. The density enhancement has characteristic dimensions L_x and L_y at $t = 0$. Since there is elongation in the y-direction and since the flow perpendicular to \vec{B} from convection is incompressible,

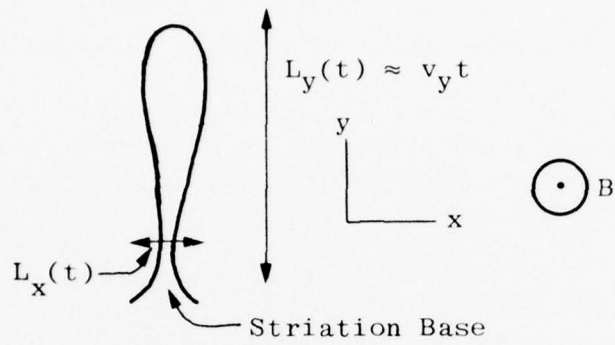
$$L_x(t) L_y(t) = L_x L_y \quad (11)$$

where $L_x(t)$ and $L_y(t)$ are characteristic dimensions in the x and y directions at time t.

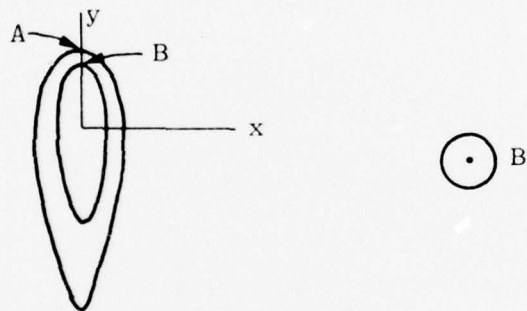
Let τ be the time when the convective velocity in the x-direction which tends to make the striation thinner in x is just balanced by the diffusive velocity in the x-direction. Then

$$\frac{\partial v_x}{\partial x} = \frac{-\partial v_y}{\partial y} \approx \frac{v_y}{L_y(\tau)}$$

a) Striation Sheet Pinching Off



b) Striation Tip Steepening



c) Striation Splintering



Figure 3. Striation Iso-Density Contours.

where v_y is the velocity of the striation tip with respect to the striation base (see Fig. 3a), assumed constant in time. Since the striation distance scale is roughly one-half the striation thickness

$$v_x \approx \frac{L_x(\tau)}{2} \frac{v_y}{L_y(\tau)} = \frac{L_x^2(\tau)}{L_x L_y} v_y \quad (12)$$

But from diffusion,

$$v_x = \frac{-1}{n} D_{\perp} \frac{\partial n}{\partial x} \approx D_{\perp} \frac{2}{L_x(\tau)} \quad (13)$$

Combining Eqs. (12) and (13) results in

$$L_x(\tau) = \left(\frac{4D_{\perp} L_x L_y}{v_y} \right)^{1/3} \quad (14)$$

The corresponding time scale is

$$\tau = \frac{[L_x(\tau)/2]^2}{D_{\perp}} = \frac{1}{(4D_{\perp})^{1/3}} \left(\frac{L_x L_y}{v_y} \right)^{2/3}$$

The dependence on D_{\perp} is not strong, but the classical time scale from Eq. (9a) is a factor of seven greater than the DDM time scale of Eq. (9b), *ceteris paribus*.

From this model for $t > \tau$ one expects $L_y(t) = v_y t$. Density decay effects can be estimated very crudely by noting that provided $L_x(t)$ is roughly constant (through diffusion) the ionization enhancement integrated a magnetic field line should decrease as

$$\tau/t, \quad t \geq \tau$$

Using $D_{\perp} = 2.5 \times 10^6$ cm²/sec, $L_x = 4 \times 10^5$ cm, $L_y = 10^6$ cm and $v_y = 10^4$ cm/sec, values which appear appropriate to the

equatorial spread F measurements of Kelley et al.⁽⁹⁾, we obtain $\tau \approx 5 \times 10^2$ sec for the time scale for density decay through diffusion and $L_x(t)/2 \approx 3 \times 10^4$ cm for the corresponding gradient scale length. A detailed comparison with experimental data could be fruitful. Mechanisms such as striation splintering would tend to decrease τ (see Fig. 3c); the effect of non-uniformity in striation thickness as a function of y (see Fig. 3a) is ambiguous.

The second situation consists of the steepening of the positive y -tip of a striation when $\partial E_x / \partial y > 0$ where E_x is the x -directed electric field at the striation tip (see Fig. 3b). These considerations could equally well apply to a "hole" being driven upward by gravity in equatorial spread F.⁽¹⁰⁾

Provided that E_x in the neighborhood of points A and B (which are separated by a distance δy along the y -axis) is generated by non-local sources it is reasonable to take

$$\frac{d(\delta y)}{dt} = \alpha \delta y \quad , \quad (15)$$

where α is independent of δy , since the relative difference in distance from a given charge source is $\delta y/L$ where L is a typical non-steepened cloud dimension. (From the one-dimensional approximation as studied in Volk and Haerendel⁽¹¹⁾, one can verify that E_x is continuous across a steep density discontinuity in y ; hence that it is not generated by local sources in y .)

The constant of proportionality α is given by

$$\alpha = \frac{c}{B} \frac{\partial E_x}{\partial y} \quad (16)$$

Now let y be the scale length for steepening. The diffusion velocity is $D_{\perp} / \delta y$. Combining this with Eqs. (15) and (16) gives:

$$\frac{D_{\perp}}{\delta y} = \frac{c}{B} \frac{\partial E_x}{\partial y} \delta y \quad (17)$$

or

$$\delta d = \left[\frac{D_{\perp}}{\frac{c}{B} \frac{\partial E_x}{\partial y}} \right]^{\frac{1}{2}} \quad (18)$$

To estimate $c/B (\partial E_x / \partial y)$ we approximate,

$$\frac{c}{B} \frac{\partial E_x}{\partial y} \approx \frac{c}{B} \frac{\mathcal{E}_x}{L}$$

where $(c/B)\mathcal{E}_x$ is one-half the velocity of the inhomogeneity with respect to ambient and L is the characteristic non-steepened dimension of the inhomogeneity. For the inhomogeneity referred to by Costa and Kelley⁽¹⁰⁾, $c\mathcal{E}_x/B \approx 8 \times 10^3$ cm/sec and $L \approx 4 \times 10^5$ cm. This yields (using DDM diffusion)

$$\delta y = \left[\frac{2.5 \times 10^6 \times 4 \times 10^5}{8 \times 10^3} \right]^{\frac{1}{2}} \approx 10^4 \text{ cm} .$$

The value from electron-ion collisional diffusion would be about 4 meters. Values which one can infer from Costa and Kelley's data⁽¹⁰⁾ are in the range 2×10^4 to 4×10^4 cm.

4. DISCUSSION

Density inhomogeneities whose field line integrated conductivities are significantly greater than ambient (a factor of 3, at least) should have time scales for decay which are at least a factor of $\sin^2 D$ (D = magnetic dip angle) lower than those for the homogeneous nighttime ionosphere provided the ambient electric field and neutral wind (as a function of altitude) are spatially constant and substantially those of the ordinary nighttime ionosphere. This effect is caused by ionization which moves downward and is not due to diffusion perpendicular to the magnetic field. Even in the absence of downward neutral winds the characteristic time for exponential decay would have as an upper bound two hours times $\sin^2 D$. For conductivities not significantly greater than ambient the time of two hours would be a more conservative estimate. (We have not considered heaved ionization which could return to the ionosphere from the magnetosphere on time scales of several hours.)

Decay of density inhomogeneities due to diffusion perpendicular to \vec{B} is strongly entwined with convective non-diffusive motion and in addition depends on whether there is collisional diffusion only or also the theoretically much stronger wave-particle scattering diffusion. The latter as we have noted can be due to drift-dissipative modes (DDM). Although possibly a matter of observational interpretation, observations of scale lengths of greater than 100 meters for ionospheric structuring^(10,12) appear to argue for a diffusion mechanism which is much stronger than electron-ion collisional diffusion.

Usage of a simple model (see Fig. 3a) which entails striation stretching linearly in time in one dimension perpendicular to the magnetic field yields a characteristic time scale for striation decay for the ionized density integrated along a magnetic field line of

$$\tau = \frac{1}{(4D_{\perp})^{1/3}} \left(\frac{L_x L_y}{|\vec{v}_{rel}|} \right)^{2/3} \quad (19)$$

where D_{\perp} is the perpendicular diffusion coefficient, \vec{v}_{rel} is the velocity of the striation tip with respect to the striation base and L_x and L_y are the striation dimensions at $t = 0$. For $t \gg \tau$, provided the striation dimension perpendicular to \vec{v}_{rel} is roughly constant as a function of time (through diffusion) the field-line integrated density variation is at τ/t . For $n_e \leq 10^6 \text{ cm}^{-3}$, the neutral density $n \lesssim 2.0 \times 10^8 \text{ cm}^{-3}$, $L_y = 4.0 \text{ km}$, $L_x = 10.0 \text{ km}$ and $|\vec{v}_{rel}| = 10^4 \text{ cm/sec}$, $\tau \approx 5 \times 10^2 \text{ sec}$ with DDM diffusion and $\tau \approx 4.0 \times 10^3 \text{ sec}$ with collisional diffusion.

Two spatial length scales appear in our estimates. The first which characterizes the x-dimension perpendicular to striation elongation is

$$L_x(\tau) = \left(\frac{4 D_{\perp} L_x L_y}{|\vec{v}_{rel}|} \right)^{1/3} \quad (14')$$

with variables as defined in Eq. (19). The second which characterizes the steepening at the tip of a striation is

$$\delta y = \left(\frac{D_{\perp} L}{c \mathcal{E}_x / B} \right)^{1/2} \quad (18')$$

Here L is the characteristic non-steepened dimension at the tip and $c \mathcal{E}_x / B$ is a measure of relative velocity within the striation prior to significant steepening which is taken to be one-half the velocity of the striation tip with respect to ambient.

Since δy corresponds to a maximum in density enhancement at the striation tip one would expect variations in the power density spectrum to be associated with it. If there are modes at relatively short wavelengths driven by large density gradients (as for instance DDM), when characteristically $\delta y = 0.1$ km, the value of Eq. (18') could mark an upper bound on their wavelengths. On the other hand, if D_{\perp} is determined by collisional effects, when characteristically $\delta y = 4$ meters, the value of Eq. (18') would mark a short wavelength cutoff to the spectrum. It is interesting to note that the estimate of Eq. (18') is very similar to that obtained through an analysis of turbulent behavior by Ott and Farley⁽¹³⁾ although the physical models appear to be different.

If D_{\perp} is determined by collisional effects, the structure of the striation tip can be found provided we assume that diffusion balances convection. Then

$$\frac{D_{\perp}}{n_e} \frac{\partial n_e}{\partial y} = \frac{-c \mathcal{E}_x y}{BL}$$

$D \sim n_e$, as with electron-ion collisions results in

$$n_e \sim c_1 - \frac{c \mathcal{E}_x y^2}{BL^2}$$

where c_1 is a constant. If D_{\perp} is independent of n_e , as when collisions with neutrals dominate,

$$n_e \sim \exp \left[-c \mathcal{E}_x y^2 / (2BLD_{\perp}) \right],$$

i.e., Gaussian behavior results. We have not found the wave spectrum at wavelengths less than δy when D_{\perp} is determined by turbulence.

5. FUTURE PRIORITIES

Work in the following areas would be useful:

1. Examination of nuclear data for evidence of spread F and decay.
2. Calculation of decay (through falling both parallel and perpendicular to B and recombination) for a striation whose conductivity is large compared to the background for disturbed nuclear conditions.
3. Calculation of decay for a striation whose conductivity is not large compared to the background through falling parallel to a field line under disturbed nuclear conditions.
4. Verification of scale lengths, observationally, for equatorial spread F and mid-latitude spread F. Checking of perpendicular diffusion coefficients through these values.
5. Determination of experimental decay behavior for equatorial spread F (which seems better understood than mid-latitude spread F) and mid-latitude spread F and determination whether stated loss mechanisms apply.
6. Further study of plasma wave phenomena - for perpendicular diffusion - and determination of the spectrum at wavelengths below δy when D_{\perp} is determined by wave turbulence.

7. It should be noted that barium cloud releases at altitudes of 200 km would tend to be stable to DDM because of the relatively higher ion-neutral collision frequency. Hence decay results from them could be misleading if applied to higher altitudes.

REFERENCES

1. M. McFarland, D. L. Albritten, F. C. Fehsenfeld, E. E. Ferguson and A. L. Schmeltpopf, "A Flow-Drift Technique for Ion Mobility and Ion-Molecule Reactor Rate Constant Measurements. 2, The Positive Ion Reaction of N^+ , O^+ and N_2^+ with O_2 and O^+ with N_2 from Thermal to 2 eV," J. Chem. Phys. 59, 6620, 1973.
2. D. F. Strobel and M. B. McElroy, "The F2 Layer at Middle Latitudes," Planet. Space Sci. 18, 1181 (1970), Figure 6.
3. This equation is based on Eq. 13 of F. W. Perkins, "Spread F and Ionospheric Currents," J. Geophys. Res. 78, 218 (1973).
4. S. R. Goldman, A. J. Scannapieco and S. L. Ossakow, "Early Time Striation Structuring in Ionized Barium Clouds Due to the Presence of B_2O Flow," NRL Memo Report 3269.
5. Private Communication with R. W. Kilb and R. Stagat.
6. M. K. Hudson, "Equatorial Spread F: Low Frequency Modes in a Collisional Plasma," Ph.D. Thesis UCLA, July 1974.

M. K. Hudson and C. F. Kennel, "The Collisional Drift Mode in a Partially Ionized Plasma," J. Plasma Phys. 14, 135 (1975).
7. K. Mauersberger, M. J. Engebretson, D. C. Kayser and W. E. Potter, "Diurnal Variation of Atomic Nitrogen," J. Geophys. Res. 81, 2413 (1976).
8. T. H. Dupree, "Non-Linear Theory of Low Frequency Instabilities," Phys. Fluids 11, 2680 (1968).
9. M. C. Kelley, G. Haerendel, H. Kappler, A. Valenzuela, B. B. Balsley, D. A. Carter, W. L. Ecklund, C. W. Carlson, B. Häusler and R. Torbert, "Evidence for a Rayleigh-Taylor Type Instability and Upwelling of Depleted Density Regions During Equatorial Spread F," Geophys. Res. Letts. 3, 448 (1976)
10. E. Costa and M. C. Kelley, "Calculations of Equatorial Scintillations at VHF and GigaHertz Frequencies Based on a New Model of the Disturbed Equatorial Ionosphere," preprint (1977).

11. H. J. Völk and G. Haerendel, "Striations in Ionospheric Ion Clouds - I.," J. Geophys. Res. 76, 4541 (1971).
12. R. K. Crane, "Spectra of Ionospheric Scintillation," J. Geophys. Res. 81, 2041 (1976).
13. E. Ott and D. T. Farley, "The k Spectrum of Ionospheric Irregularities," J. Geophys. Res. 79, 2469 (1974).

APPENDIX A. CONVECTIVE MOTION PERPENDICULAR TO \vec{B}
THROUGH ELECTRIC POLARIZATION

Using a waterbag model⁽⁴⁾:

$$\Sigma = \Sigma_1, \quad \rho < \rho_0; \quad \Sigma = \Sigma_2, \quad \rho > \rho_0 \quad (\text{A-1})$$

$$N = N_1, \quad \rho < \rho_0; \quad N = N_2, \quad \rho > \rho_0 \quad (\text{A-2})$$

where ρ is the cylindrical radius around the axis in the direction of $\vec{B}/|\vec{B}|$, from Eq. (6) we have,

$$\nabla_{\perp}^2 \psi = 0, \quad \rho < \rho_0 \quad (\text{A-3})$$

$$\nabla_{\perp}^2 \psi = 0, \quad \rho > \rho_0 \quad (\text{A-4})$$

Using e_{ρ} as the unit radial vector and e_{θ} as the unit azimuthal vector,

$$\nabla_{\perp} \psi \cdot e_{\theta} \Big|_{\rho_0 - \epsilon} = \nabla_{\perp} \psi \cdot e_{\theta} \Big|_{\rho_0 + \epsilon}, \quad \epsilon \ll \rho_0 \quad (\text{A-5})$$

and

$$\begin{aligned} \Sigma_1 E_0 + \frac{\mathbf{v} \times \mathbf{B}}{c} - \nabla_{\perp} \psi \cdot e_{\rho} + N_1 \frac{e_{\theta} \times \vec{B}}{\omega_{ci} |\mathbf{B}|} \cdot e_{\rho} \Big|_{\rho_0 - \epsilon} \\ = \Sigma_2 E_0 + \frac{\mathbf{v} \times \mathbf{B}}{c} - \nabla_{\perp} \psi \cdot e_{\rho} + N_2 \frac{e_{\theta} \times \vec{B}}{\omega_{ci} |\mathbf{B}|} \cdot e_{\rho} \Big|_{\rho_0 + \epsilon} \end{aligned} \quad (\text{A-6})$$

The solutions have the form,

$$\psi = \sum_{n=1}^{\infty} \left[a_{nc} \rho^n \cos n\theta + a_{ns} \rho^n \sin n\theta \right], \quad \rho < \rho_0 \quad (\text{A-7})$$

$$\psi = \sum_{n=1}^{\infty} \left[b_{nc} \rho^{-n} \cos n\theta + b_{ns} \rho^{-n} \sin n\theta \right], \quad \rho > \rho_0 \quad (\text{A-8})$$

From Eq. (A-5),

$$b_{nc} = \rho_0^{2n} a_{nc}, \quad b_{ns} = \rho_0^{2n} a_{ns}.$$

From Eq. (A-6),

$$\begin{aligned} \Sigma_1 \nabla_{\perp} \psi \cdot e_{\rho} \Big|_{\rho_0 - \epsilon} - \Sigma_2 \nabla_{\perp} \psi \cdot e_{\rho} \Big|_{\rho_0 + \epsilon} &= (\Sigma_1 - \Sigma_2) \left(\frac{E_0 + v \times B}{c} \right) \cdot e_{\rho} \\ &+ (N_1 - N_2) e \frac{\vec{g} \times B \cdot e_{\rho}}{\omega_{ci} |B|} \end{aligned}$$

Define, with \hat{e}_x the unit vector in direction of \vec{A} ,

$$\vec{A} = A \hat{e}_x = E_0 + \frac{v \times B}{c} + \frac{(N_1 - N_2)}{(\Sigma_1 - \Sigma_2)} \frac{e \vec{g} \times B}{\omega_{ci} |B|}$$

We have,

$$\Sigma_1 \nabla_{\perp} \psi \cdot e_{\rho} \Big|_{\rho_0 - \epsilon} - \Sigma_2 \nabla_{\perp} \psi \cdot e_{\rho} \Big|_{\rho_0 + \epsilon} = (\Sigma_1 - \Sigma_2) A \cdot e_{\rho}$$

or

$$\left(\Sigma_1 a_{1c} + \Sigma_2 \frac{b_{1c}}{\rho_0^2} \right) \cos \theta = (\Sigma_1 - \Sigma_2) A \cos \theta.$$

Then

$$a_{1c} = \frac{(\Sigma_1 - \Sigma_2) A}{\Sigma_1 + \Sigma_2}$$

and

$$\psi = a_{1c} x.$$

Hence ,

$$-\nabla_{\perp}\psi = -\hat{e}_x a_{1c} = \frac{(\Sigma_2 - \Sigma_1)\vec{A}}{\Sigma_1 + \Sigma_2}$$

and,

$$v_{\perp} = \frac{c E \times B}{B^2}$$

or

$$v_{\perp} = \frac{c E_{\perp 0} \times B}{B^2} \frac{2\Sigma_2}{\Sigma_1 + \Sigma_2} + \frac{c}{B^2} \frac{(\Sigma_2 - \Sigma_1)}{\Sigma_1 + \Sigma_2} \left[\frac{(v \times B) \times B}{c} + \frac{(N_1 - N_2)}{\Sigma_1 - \Sigma_2} \frac{e(g \times B) \times B}{\omega_{ci} |B|} \right] .$$

PART 2

A SYNOPSIS OF DRIFT MODE BEHAVIOR

CONTENTS

	<u>Page</u>
1. INTRODUCTION	2-3
2. BASIC MECHANISM FOR NEUTRALLY STABLE DRIFT WAVE	2-5
2.1 Characteristics of Background Plasma	2-5
2.2 Mode Structure	2-5
3. INSTABILITY MECHANISM FOR DRIFT WAVES	2-8
3.1 Equivalence of $\sin \Delta > 0$ and Net Flux Against Background Density Gradient	2-8
3.2 Relation between γ and $\sin \Delta$	2-10
3.3 Equivalence of $\omega_r - kv_{De} < 0$ and $ \omega_r - kv_{De} \ll \omega_r$ with Instability	2-10
3.4 Ion Behavior	2-11
4. RELATION TO OTHER TYPES OF DRIFT MODES	2-13
5. GROWTH RATES AND PARAMETER RANGES FOR DRIFT DISSIPATIVE MODES	2-14
6. DIFFUSION COEFFICIENT FROM DRIFT-DISSIPATIVE MODES; ADDITIONAL PHYSICAL EFFECTS	2-17
7. SUMMARY	2-20
REFERENCES	2-21

1. INTRODUCTION

Drift modes are of interest in HANE behavior because they furnish a mechanism in addition to the usual $E \times B$ instability⁽¹⁾ which can affect the structuring and possible decay of highly elongated striations (which themselves are most likely due to $E \times B$ modes). Decay of $E \times B$ modes into drift modes is a possible source of the k^{-2} power density spectrum.⁽²⁾ (k is modal wave number in direction of observation, which we will take to be the y-direction, B is in the z-direction, and ∇n is in the x-direction.) In addition it has been shown⁽³⁾ that scale lengths of 0.1-0.2 km at striation tips can be attributed to drift wave turbulence. (These structures are believed responsible for anomalous gigahertz scintillation.⁽⁴⁾)

For the geometry described in the paragraph above, with E predominantly in the x-direction, striations tend to elongate in the y-direction. $E \times B$ mode growth may be strong at the striation tips where one expects $|\vec{E} \times \nabla n|/|\vec{E} \cdot \nabla n| \gg 1$. However along the elongated striation sides one expects $|E \times \nabla n|/|E \cdot \nabla n| \ll 1$. It is then highly likely that $E \times B$ instability is suppressed by the non-existence of localized $E \times B$ normal modes.⁽⁵⁾ (We note that the x and y directions in Ref. 5 are interchanged with those used here.) Drift modes provide an additional instability mechanism which is not necessarily suppressed when $|E \times \nabla n|/|E \cdot \nabla n| \ll 1$. Hence it is possible that the resulting plasma turbulence could result in the decay of striations even when $E \times B$ turbulence is not indicated.

Within this paper we present results which show that drift wave instability is definitely not limited by $E \cdot \nabla n$

provided $Lc|E \cdot \nabla n|/(B|\nabla n|) \leq 2 \times 10^7 \text{ cm}^2/\text{sec}$. (Here $L = |(n^{-1} dn/dx)^{-1}|$.) At larger values of $Lc|E \cdot \nabla n|/(B|\nabla n|)$ behavior has not yet been firmly established.

We intend for this synopsis to serve as an introduction to drift waves as they apply to striation decay in the ionosphere and as used in Ref. 3. We first present a physical picture of neutrally stable drift waves and then indicate the instability mechanism. We next show the connection between the collisionless drift instability (universal instability) and the drift-dissipative instability. For a variety of ionospheric conditions we then present drift-dissipative modal growth rates and frequencies with logarithmic perpendicular density gradients, equal to $(n^{-1} dn/dx)$, a factor of 2.5 above the minimum logarithmic perpendicular density gradients producing marginal stability. (Mode parameters k_z and k are the same as at marginal stability; modes vary as $\exp(-i\omega t + ik_z z +iky)$.) We then find a simple form for a lower bound on the growth rate for drift-dissipative instability to be used in diffusion estimates. Next drift dissipative eigenmode structure is investigated for use in diffusion coefficients and the origin of the diffusion coefficient $D = 0.07 C_s^2/\omega_{ci}$ used in Ref. 3 is indicated. ($C_s = \{k_b(T_i + T_e)/m_i\}^{1/2}$, $k_b =$ Boltzmann's constant, $T =$ temperature, $m =$ mass, $i =$ ion quantity, $e =$ electron quantity, $\omega_c =$ cyclotron frequency.) Finally the possibility of drift wave modification when $E \cdot \nabla n/|\nabla n|$ is sufficiently large, $\{(Lc|E \cdot \nabla n|/B|\nabla n|) \geq 2 \times 10^7 \text{ cm}^2/\text{sec}\}$, is indicated, and the relative weakness of electromagnetic effects for drift-dissipative modes as contrasted to collisionless drift modes is demonstrated.

2. BASIC MECHANISM FOR NEUTRALLY STABLE DRIFT WAVE*

2.1 CHARACTERISTICS OF BACKGROUND PLASMA

Electron temperature is T_e , electrons are able to move along magnetic field lines, background density is n , density gradient is $\partial n / \partial x$.

2.2 MODE STRUCTURE

Modal quantities are indicated by subscript "1", variation in y and z , electrostatic, quasi-neutral, density (n_1) and potential (ϕ_1) $\propto \exp(iky + ik_z z - i\omega t)$. Electrons and ions are treated as fluids.

Therefore velocities are:

$$v_{1\perp} = v_{1e\perp} = v_{1i\perp}$$

or

$$v_{1\perp} = cE_{1y} \hat{i} / B = -ik c \phi_1 / B \hat{i} \quad (1)$$

and

$$v_{1ez} = -\frac{q E_{1z}}{m_e \nu_e} - \frac{k_b T_e}{m_e \nu_e} \frac{1}{n} \frac{\partial n_1}{\partial z} \quad (2)$$

(with ν_e the sum of electron-neutral and electron-ion collision frequencies, $\nu_e = \nu_{en} + \nu_{ei}$). Diffusion velocity perpendicular to \vec{B} is neglected since it does not contribute to the density equations, Eqs. (3) and (4).

For ions with no motion parallel to \vec{B} ,

$$\frac{\partial n_1}{\partial t} + v_{1\perp} \cdot \nabla n = 0 \quad (3)$$

We note $\nabla \cdot v_{1\perp} = 0$ for $\nabla \times E_1 = 0$ (electrostatic modes).

*The discussion of this section and of Section 3 is patterned after Reference 6.

For electrons

$$\frac{\partial n_1}{\partial t} + v_1 \cdot \nabla n + n \nabla \cdot v_1 = 0 \quad (4)$$

or subtracting Eq. (3) from Eq. (4),

$$\nabla \cdot v_1 = \partial v_{1z} / \partial z = 0 \quad (5)$$

From Eqs. (2) and (5),

$$\frac{q\phi_1}{k_B T_e} = \frac{n_1}{n} \quad (6)$$

Substituting Eq. (6) into Eq. (3) and using Eq. (1) results in

$$\frac{\omega}{k} = - \frac{c}{qB} k_B T_e \frac{1}{n} \frac{\partial n}{\partial x} \equiv v_{De} \quad ,$$

i.e., waves move at electron diamagnetic velocity, v_{De} , and are neutrally stable. For thermal equilibrium for electrons,

$$\frac{n + n_1}{n} = \exp(-q_e \phi_1 / k_B T_e) \quad ,$$

with q_e ($= -q$) the electron charge. For $q\phi_1 / k_B T_e \ll 1$ this is the same as

$$\frac{n_1}{n} = \frac{q\phi_1}{k_B T_e} \quad .$$

Hence the electrons are in thermal equilibrium.

Further, since n_1 is in phase with ϕ_1 and $E_1 = -\nabla\phi_1 = -ik\phi_1$, Fig. 1 is appropriate. Referring to Fig. 1 the flux in the x-direction is

$$n_1 c \frac{E_1 \times B}{B^2} = \frac{kc}{B} |n_1| |\phi_1| \cos(ky + k_z z - \omega t) \sin(ky + k_z z - \omega t) \quad .$$

Integrating over one wavelength in the y-direction gives zero, i.e., no net transport of density.

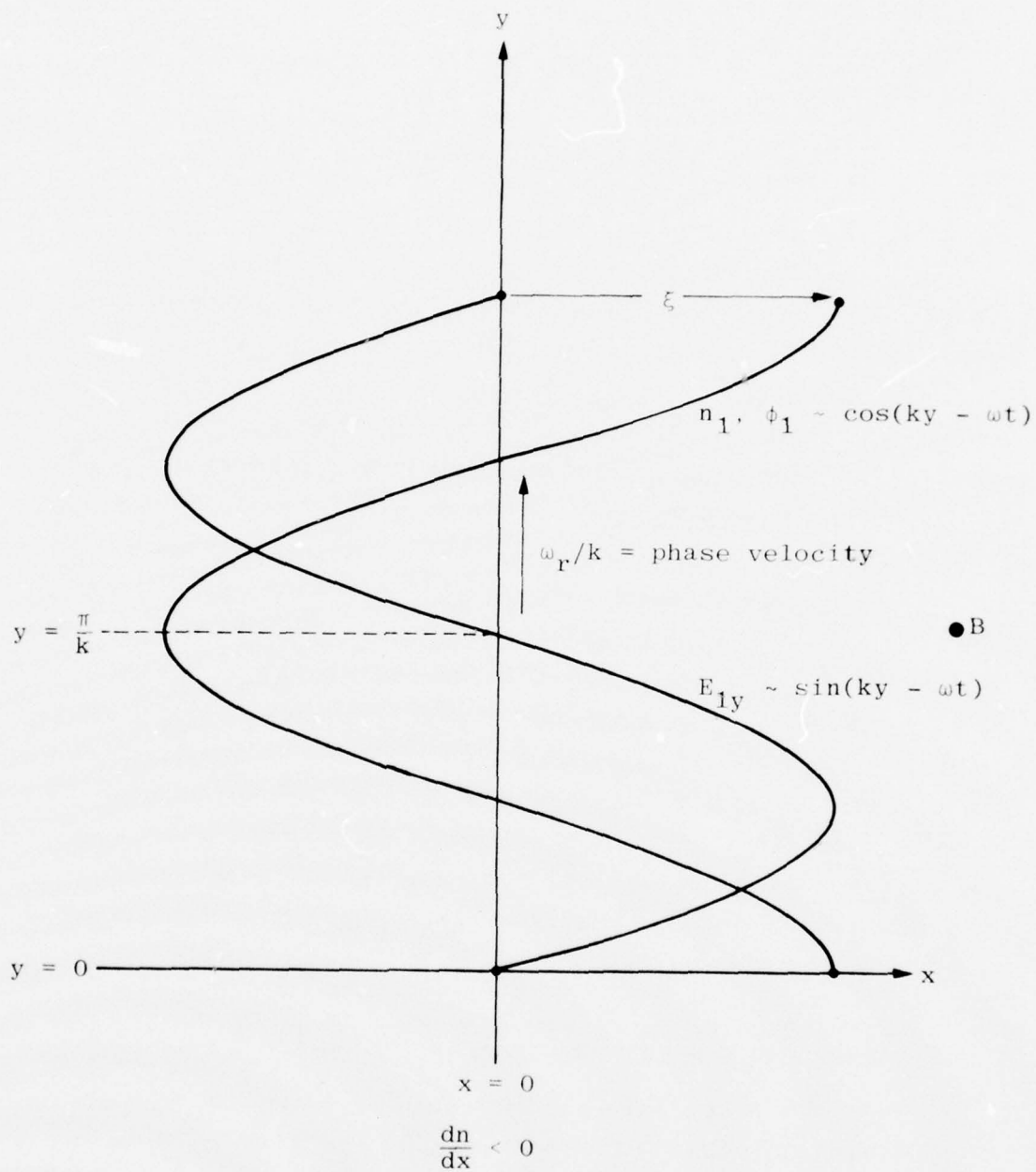


Figure 1. Relationships for a Neutrally Stable Drift Mode, $\omega_r/k = v_{De}$. Phase velocity is in positive y direction, $t = 0$, $z = 0$.

3. INSTABILITY MECHANISM FOR DRIFT WAVES

Instability of drift waves for a fluid plasma can be viewed as driven by deviations in the ion fluid behavior from that described in Eqs. (1) and (3). Drift modes are unstable when $\omega_r < kv_{De}$ and $|\omega - kv_{De}|/kv_{De} \ll 1$. (Here ω_r is the real part of ω ($\omega \equiv \omega_r + i\gamma$)). Then ϕ_1 lags n_1 in phase along the direction of wave propagation and there is a mean fluid flux, corresponding to instability, which acts to decrease the background density gradient by transporting fluid from higher to lower background densities. Hence effects which act to reduce ω_r act to produce instability. Two such effects are ion inertia and finite ion Larmor radius corrections.

On defining Δ/k to be the distance that ϕ_1 lags behind n_1 in the direction of wave propagation, the condition $\sin \Delta > 0$ is equivalent to a net flux against the background density gradient. We first show that $\gamma \approx kv_{De} \sin \Delta$, then that $\omega_r - kv_{De} < 0$ corresponds to $\gamma > 0$ (and that $\omega_r - kv_{De} > 0$ corresponds to $\gamma < 0$). Finally we introduce ion behavior and show how it can change ω .

3.1 EQUIVALENCE OF $\sin \Delta > 0$ AND NET FLUX AGAINST BACKGROUND DENSITY GRADIENT

When the potential lags the density by a distance Δ/k in the direction of wave propagation the geometry is as shown in Fig. 2. The potential is represented as $\phi_1 = |\phi_1| \exp(iky + ik_z z - i\omega_r t + i\Delta)$ and the density is $n_1 = |n_1| \exp(iky + ik_z z - i\omega_r t)$. On taking real parts of $E_1 = -\nabla\phi_1$ and n_1 the flux is

$$cn_1 E_1 \times B/B^2 = |n_1| |\phi_1| kc \{ \sin(ky + k_z z - \omega_r t) \cos \Delta + \cos(ky + k_z z - \omega_r t) \sin \Delta \} \cos(ky + k_z z - \omega_r t) .$$

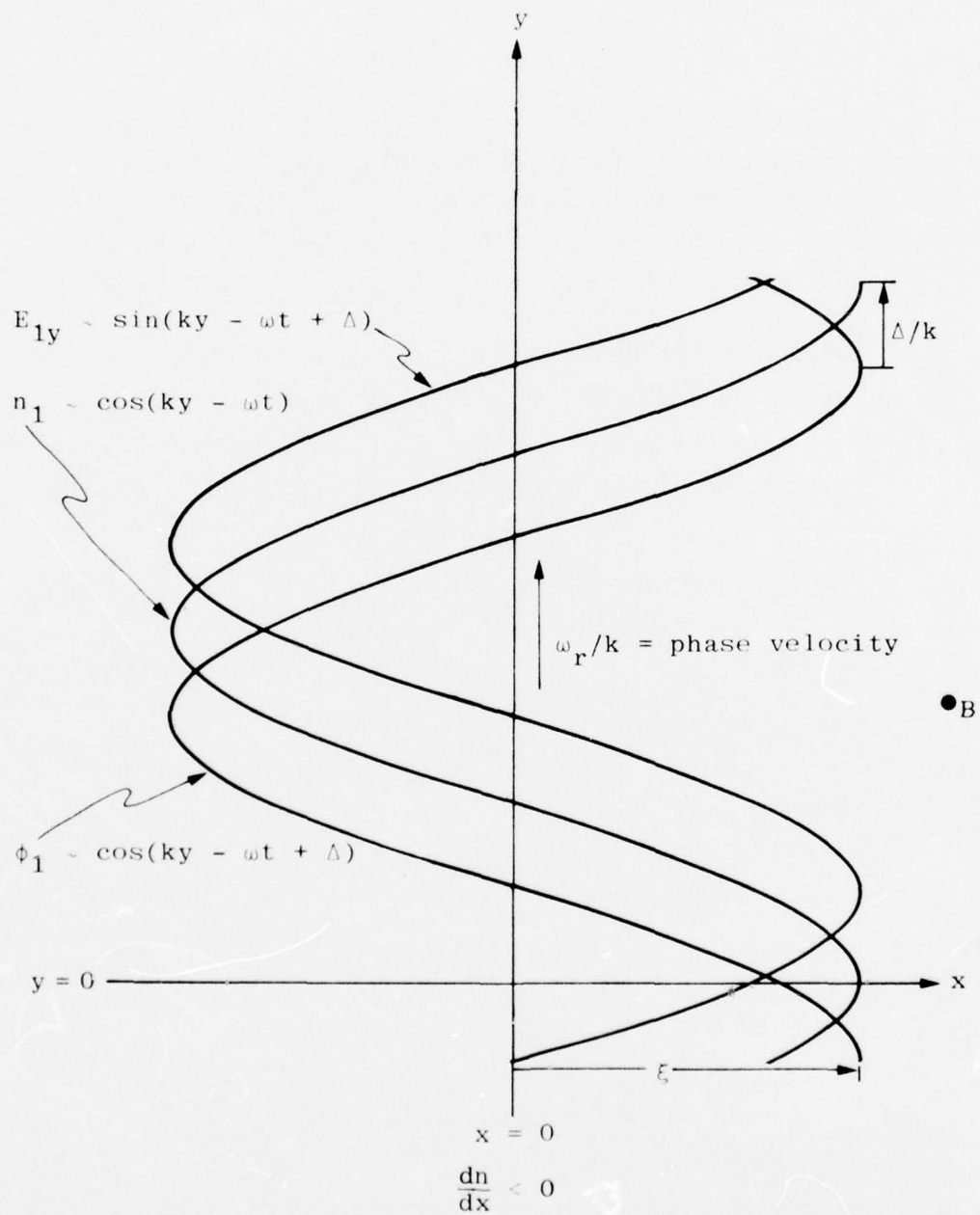


Figure 2. Relationships for an Unstable Drift Mode, $0 < \omega_r/k < v_{De}$. ϕ_1 lags n_1 along the direction of wave phase velocity (positive y-direction) by $\pi/4k$ ($\Delta = \pi/4$), $t = 0$, $z = 0$.

On averaging over wavelength, with $\langle \rangle$ denoting the average and t fixed, this results in

$$\langle n_1 v_{1x} \rangle = |n_1| |\phi_1| kc \sin \Delta / 2B \quad , \quad (7)$$

i.e., fluid flux in the positive x -direction, against the background density gradient. (Alternately from Fig. 2, remembering that B is in the positive z direction, one can easily see that the density extremes at $y = 0$ and $y = \pi/k$ move farther away from $x = 0$ when $\Delta > 0$.)

3.2 RELATION BETWEEN γ AND $\sin \Delta$

On the other hand if the ion flow is given to first approximation by Eq. (1) and ξ denotes the displacement of the ion density perturbation from $x = 0$ (see Fig. 1 or Fig. 2) one has

$$n_1 = - \xi \, dn/dx$$

and

$$v_{1x} = d\xi/dt \quad .$$

On taking $\xi \propto e^{\gamma t} \cos(ky + k_z z - \omega_r t)$ and averaging over a period in time one has

$$n_1 v_{1x} = - \gamma |n_1|^2 / (2 \, dn/dx) \quad . \quad (8)$$

On using Eq. (6) as a first approximation for $|n_1|/|\phi_1|$ and equating Eqs. (7) and (8) this results in:

$$\gamma = kv_{De} \sin \Delta \quad . \quad (9)$$

3.3 EQUIVALENCE OF $\omega_r - kv_{De} < 0$ AND $|\omega_r - kv_{De}| \ll \omega_r$ WITH INSTABILITY

To show the stated equivalence we first note from Eqs. (1), (2) and (4)

$$\frac{n_1}{\phi_1} = \frac{qn}{k_b T_e} \left(\frac{ikv_{De} - \delta}{i\omega - \delta} \right), \quad (10)$$

with $\delta = k_z^2 k_b T_e / m_e v_e$. Using Eq. (6) again to approximate $|n_1|/|\phi_1|$, Eq. (9), noting $\omega \equiv \omega_r + i\gamma$ and taking the imaginary part of Eq. (10) results in (after some algebra),

$$\gamma = \frac{kv_{De} \delta(\omega_r - kv_{De})}{(kv_{De})^2 - \omega_r^2 - (\gamma + \delta)^2} \approx \frac{-kv_{De} \delta(\omega_r - kv_{De})}{(\gamma + \delta)^2},$$

hence the equivalence.

3.4 ION BEHAVIOR

Ion behavior within drift waves has been calculated by Kennel and Hudson.⁽⁷⁾ Their result yields

$$\frac{n_1/n}{q\phi_1/kT_e} = \frac{\omega_{De} - b\omega - iv_{\perp}}{\omega + R_T b(\omega + iv_{\perp}/b)}, \quad (11)$$

where $b = k^2 k_b T_e / (m_i \omega_{ci}^2)$, $R_T \approx T_i / T_e$ and $v_{\perp} = b(v_{in} + 0.3bv_{ii}) \equiv bv_i$. (v_{in} is the ion-neutral collision frequency; v_{ii} the ion-ion collision frequency.) It can readily be verified that Eqs. (10) and (11) combine to give Eq. (1b) of Ref. 7. On the right-hand side of Eq. (11), the contribution $-b\omega$ in the numerator is due to ion inertia and the contribution linear in $R_T b$ in the denominator is due to finite ion Larmor radius effects. For large electron conductivity parallel to \vec{B} one has $\delta \gg \omega, kv_{De}$. Then one obtains $(n_1/n)/(q\phi_1/kT_e) \approx 1$ and one sees that both ion inertia ($-b\omega$) and the finite ion Larmor radius term ($R_T b\omega$) act to decrease ω , hence to cause ϕ_1 to lag behind n_1 in the direction of wave propagation, hence to drive instability. Under the same conditions it is easy to see that collisional contributions in v_{\perp} are stabilizing.

We note that the fluid results appear somewhat uncertain in detail in that in calculations which we carried out there were discrepancies from Eq. (11). However, our discrepancies were of such magnitude and sign as to enhance the instability, so that the results presented below, which are based on Eq. (11), are from that standpoint at worst conservative as concerns the effect of the instability.

4. RELATION TO OTHER TYPES OF DRIFT MODES

Combination of Eqs. (10) and (11) is also in agreement with the Vlasov result appropriate to each species, α , governed by the equation,

$$\left(\frac{\partial}{\partial t} + \mathbf{v} \cdot \frac{\partial}{\partial \mathbf{r}} + \frac{q_\alpha}{m_\alpha} \mathbf{v} \times \mathbf{B} \cdot \frac{\partial}{\partial \mathbf{v}} \right) f_{1\alpha} = i \frac{q_\alpha}{m_\alpha} \phi \mathbf{k} \wedge \frac{\partial f_{0\alpha}}{\partial \mathbf{v}} - v_\alpha \left(f_{1\alpha} - \frac{n_{1\alpha}}{n_0} f_0 \right)$$

with quasi-neutrality, provided with $v_{T\alpha} = (k_B T_\alpha / m_\alpha)^{1/2}$ one takes $\omega \sim v_i \gg k_z v_{Ti}$, $v_e \gg k_z v_{Te}$, and $v_e \gg \omega$.⁽¹¹⁾ The inequality $v_e \gg \omega$ corresponds to the drift-dissipative mode for which contributions involve the plasma dispersion function W in the form

$$W \left(\frac{\omega + i v_e - n \omega_{ce}}{\sqrt{2} k_z v_{Te}} \right)$$

with n a running integer index. The collisionless "universal instability" is based on $v_e \ll \omega$, $v_i \ll \omega$, $v_{Ti} \ll \omega/k_z \ll v_{Te}$.⁽⁹⁾

For $T_e = 0.1$ eV and $10^3 < n_e < 10^6$ cm⁻³ we have $v_{ei} \approx 1.5 n_e / 10^3$, and the limit $v_e \gg \omega$ seems generally reasonable. The limit $v_e \gg \sqrt{2} k_z v_{Te}$ is the isothermal limit of Hudson and Kennel.⁽⁷⁾ Comparison of their Figs. 2 and 3 indicates agreement between the isothermal limit and finite heat conduction drift modes within a factor of about 3.

5. GROWTH RATES AND PARAMETER RANGES FOR
DRIFT DISSIPATIVE MODES

The growth rates and general modal behavior stated below are subject to a number of uncertainties involving the precise form for electron and ion behavior as well as usage of fluid results for b comparable to unity. A major justification for presenting the results is that in many cases the diffusion coefficient derived from them can be much larger than that resulting from coulomb collisions.⁽³⁾

Combination of Eqs. (10) and (11) and solving for $\omega \equiv \omega_r + i\gamma$ (ω_r = resonant frequency, γ = growth rate) results in

$$\gamma = \frac{1}{2} \left\{ -\tau + \frac{\sqrt{2}}{2} \left[A + (A^2 + B^2)^{\frac{1}{2}} \right]^{\frac{1}{2}} \right\} \quad (12)$$

and

$$\omega_r = \frac{1}{2} \left\{ -\frac{yz}{2} + \frac{\sqrt{2}}{2} \left[(A^2 + B^2)^{\frac{1}{2}} - A \right]^{\frac{1}{2}} \right\} \quad (13)$$

where

$$\tau = 1 + x(1 + y^2)$$

$$A = \tau^2 - 4xy^2 - (yz/2)^2$$

$$B = 2xyz \left[1 + (1 + y^2)/2 \right] - yz$$

$$x = \frac{k_z^2}{k^2} \frac{\omega_{ci} \omega_{ce}}{v_i v_e}$$

$$y = kC_s / \omega_{ci}$$

$$z = C_s / (Lv_i)$$

The condition $\gamma = 0$ relates x , y and z at marginal stability. Regarding z as a function of the independent variables x and y and minimizing z successively with respect to x and y results in three equations for x , y and z . Hence for given ionized density, neutral density and ionospheric temperatures it is possible to find the largest value of L ($= L^*$) at which there can be instability and the corresponding values of x , y and z .

In Table 1, restricting wavelengths along the magnetic field to less than 100 km, for variable electron density (NE) and neutral density (NEUT) with $L = 0.4L^*$ and $T_e = T_i = 0.1$ eV, we have presented γ (RATE) and ω_r (FREQ) for values of x and y close to those which resulted in L^* but with $L = 0.4L^*$, i.e., we present results appropriate to marginally stable parameters but with spatial gradients a factor of 2.5 above marginal stability (LPERP represents L).

It is clear that there are numerous cases of unstable behavior with L on the scale of tenths of a kilometer with $kL \gg 1$. (We note that the condition $kL > 5$ is the same as $Ly > 2 \times 10^3$ (L in cm).)

A simple expression for the growth rate obtains for $x = z \gg 1$, with $y = 1$. One finds

$$\gamma = 0.07 C_s/L \quad . \quad (14)$$

The result is significant because it furnishes a lower bound on growth rates which can be used in expressions for the diffusion coefficient. The value $y = 1$ is at the limit of validity of fluid plasma calculations ($y < \sqrt{2}$) but calculations in which the ions are treated by the Vlasov equation, collisionlessly, but with y arbitrary yield a similar result.

Table I. Drift Mode Parameters. For fixed ionospheric neutral density (NEUT) in cm^{-3} and ionized density (NE) in cm^{-3} there is some value of $L (= L^*)$ in cm above which instability does not occur and a neutrally stable mode (specified by kz and k) at L^* . This table shows the modal growth rate (RATE) in sec^{-1} and oscillation frequency (FREQ) in sec^{-1} with the same kz and k but with $L = 0.4 L^*$ (LPERP), i.e., with density gradient 2.5 greater than the smallest unstable density gradient for the specified ionospheric conditions of each row. Electron and ion temperatures are both 0.1 eV. $x = kZ$, $y = kC_s/\omega_{ci}$, $z = C_s/Lv_i$.

NE	NEUT	LPERP	X	Y	Z	RATE	FREQ
1.0E+4	1.0E+6	6.739E+4	1.555E+4	4.369E-1	5.016E+2	2.178E-3	2.382E-1
1.0E+4	1.0E+7	4.130E+4	1.247E+3	6.947E-1	1.663E+2	2.164E-2	4.944E-1
1.0E+4	1.0E+8	1.759E+4	9.860E+1	9.178E-1	5.483E+1	1.987E-1	1.165E+0
1.0E+4	1.0E+9	5.704E+3	7.840E+0	9.893E-1	1.829E+1	1.084E+0	2.205E+0
(1.0E+4	1.0E+10	9.872E+2	2.500E+0	3.551E-1	1.068E+1	2.091E+0	4.549E+0)
1.0E+5	1.0E+6	8.311E+4	1.739E+3	2.547E-1	1.546E+2	2.175E-3	1.258E-1
1.0E+5	1.0E+7	6.682E+4	1.555E+2	4.369E-1	5.059E+1	2.106E-2	2.342E-1
1.0E+5	1.0E+8	3.761E+4	1.247E+1	6.947E-1	1.826E+1	1.392E-1	3.872E-1
1.0E+5	1.0E+9	8.715E+3	2.500E+0	5.914E-1	1.165E+1	3.691E-1	6.087E-1
(1.0E+5	1.0E+10	1.029E+3	2.500E+0	1.761E-1	1.025E+1	7.710E-1	2.802E+0)
1.0E+6	1.0E+6	8.895E+4	1.814E+2	1.449E-1	4.876E+1	2.159E-3	6.895E-2
1.0E+6	1.0E+7	7.661E+4	1.739E+1	2.547E-1	1.678E+1	1.885E-2	1.168E-1
1.0E+6	1.0E+8	3.787E+4	2.500E+0	3.782E-1	1.076E+1	5.831E-2	1.220E-1
(1.0E+6	1.0E+9	9.880E+3	2.500E+0	1.886E-1	1.027E+1	8.944E-2	3.073E-1)
(1.0E+6	1.0E+10	1.042E+3	2.500E+0	6.026E-2	1.012E+1	1.096E-1	1.065E+0)
1.0E+7	1.0E+6	8.482E+4	1.840E+1	8.177E-2	1.652E+1	2.045E-3	3.741E-2
1.0E+7	1.0E+7	4.980E+4	2.500E+0	1.335E-1	1.019E+1	1.002E-2	4.621E-2
1.0E+7	1.0E+8	4.005E+4	2.500E+0	1.196E-1	1.017E+1	1.027E-2	5.227E-2
1.0E+7	1.0E+9	1.002E+4	2.500E+0	5.968E-2	1.012E+1	1.117E-2	1.096E-1
1.0E+7	1.0E+10	1.043E+3	2.500E+0	1.922E-2	1.011E+1	1.147E-2	3.449E-1
1.0E+8	1.0E+6	5.130E+4	2.500E+0	4.268E-2	1.011E+1	1.134E-3	1.546E-2
1.0E+8	1.0E+7	5.017E+4	2.500E+0	4.221E-2	1.011E+1	1.135E-3	1.563E-2
(1.0E+8	1.0E+8	4.029E+4	2.500E+0	3.782E-2	1.011E+1	1.138E-3	1.748E-2)
(1.0E+8	1.0E+9	1.004E+4	2.500E+0	1.887E-2	1.011E+1	1.149E-3	3.520E-2)
(1.0E+8	1.0E+10	1.043E+3	2.500E+0	6.084E-3	1.010E+1	1.152E-3	1.094E-1)
(1.0E+9	1.0E+6	5.134E+4	2.500E+0	1.350E-2	1.010E+1	1.151E-4	4.927E-3)
(1.0E+9	1.0E+7	5.021E+4	2.500E+0	1.335E-2	1.010E+1	1.151E-4	4.982E-3)
(1.0E+9	1.0E+8	4.032E+4	2.500E+0	1.196E-2	1.010E+1	1.151E-4	5.561E-3)
(1.0E+9	1.0E+9	1.004E+4	2.500E+0	5.969E-3	1.010E+1	1.152E-4	1.115E-2)
(1.0E+9	1.0E+10	1.043E+3	2.500E+0	1.924E-3	1.010E+1	1.153E-4	3.459E-2)

6. DIFFUSION COEFFICIENT FROM DRIFT-DISSIPATIVE
MODES; ADDITIONAL PHYSICAL EFFECTS

The diffusion coefficient resulting from drift-dissipative modes has been stated to be roughly γ/k_x^2 where k_x is a wave number corresponding to the modal spatial extent in the x-direction.⁽¹⁰⁾ Hence to estimate diffusion it was necessary to consider the eigenmode equation for drift modes. We have obtained eigenmode equations with collisional electrons ($v_e \gg k_z v_{Te}$, ω) and either fluid ions or collisionless ions with no restriction to $y < 1$. Although there is some uncertainty as to the precise form of the coefficients, for both cases there is an eigenvalue equation of the general form

$$\frac{d^2 \phi_1}{dx^2} + \frac{B}{\rho_i} \{n(x), L(x), v_e L / \rho_i C_S\} \phi_1 = 0 \quad , \quad (15)$$

with B of order unity, $\rho_i = (k_b T_i / m_i)^{1/2} \omega_{ci}^{-1}$, and $v_e = cE \cdot \nabla n / (B |\nabla n|)$.

For $L v_e / (\rho_i C_S) \ll 1$ we have $B = B\{n(x), L(x), 0\}$ and Eq. (15) has the form

$$\frac{d^2 \phi_1}{dx^2} + \frac{1}{\rho_i} \left[B(x_0) + \frac{dB}{dx}(x_0)(x - x_0) + \frac{1}{2} \frac{d^2 B}{dx^2}(x - x_0)^2 \right] \phi_1 = 0 \quad , \quad (16)$$

with

$$\frac{dB}{dx} \sim \frac{B}{L} \quad \text{and} \quad \frac{d^2 B}{dx^2} \sim \frac{B}{L^2}$$

Following the analysis of Ref. 5, see especially Eq. (4), we have $B \sim \rho_i^2 \approx a \sim$ so that $k_x \approx (a \sim)^{1/2} \approx (L \rho_i)^{-1/2}$. Together with Eq. (14) this leads to

$$D = \gamma/k_x^2 = 0.07 C_S^2/\omega_{ci} \quad .$$

Using $C_S = 7 \times 10^4$ cm/sec and $\rho_i = 3 \times 10^2$ cm, one finds that $Lv_\epsilon/(C_S\rho_i) < 1$ and hence that electric fluid modifications are not significant for

$$Lv_\epsilon < 2.1 \times 10^7 \text{ cm}^2/\text{sec} \quad .$$

Thus for $v_\epsilon = 10^3$ cm/sec, one requires $L < 2.1 \times 10^4$ cm for drift modes without significant plasma velocity shear modification, and for $v_\epsilon = 10^4$ cm/sec, one requires $L < 2.1 \times 10^3$ cm for the same. The use of this inequality is not meant to indicate any tendency for shear to inhibit drift modes when the inequality is not satisfied. It does indicate that drift-mode turbulence estimates at the tips of striations where $v_\epsilon \approx 0$ are on a stronger theoretical ground than those along the sides of striations where $v_\epsilon \neq 0$. Locations where $v_\epsilon \approx 0$ are thought to be the sources of anomalous gigahertz scintillation.⁽⁴⁾ Behavior for $Lv_\epsilon/(\rho_i C_S) \geq 1$ is currently under investigation.

A final point concerns the limitation of the parametric range for drift mode instability due to electromagnetic coupling effects. Collisionless drift modes are modified when β , the ratio of plasma pressure to magnetic field pressure, is greater than m_e/m_i .⁽⁹⁾ We find for drift-dissipative modes that there is not significant electromagnetic modification unless $\beta > (m_e v_e)/(m_i C_S/L)$.

Electromagnetic behavior arises because of the contribution of the modal electron current along the background magnetic field lines to the modal magnetic field. The electron current varies as the electron fluid velocity parallel to \vec{B} . Hence we have,

$$\frac{\partial v_{1ze}}{\partial t} + \nu_e v_{1ze} = - \frac{qE_{1z}}{m_e} - \frac{k_b T_e}{m_e} \frac{1}{n} \frac{\partial n_1}{\partial z} ,$$

or,

$$v_{1ze} = \frac{1}{(-i\omega + \nu_e)} \left(- \frac{qE_{1z}}{m_e} - \frac{k_b T_e}{m_e} \frac{1}{n} \frac{\partial n_1}{\partial z} \right) .$$

Hence the magnetic field source term is a factor ω/ν_e lower for the drift-dissipative mode than it would be in the absence of electron collisions, and it is plausible that the threshold for electromagnetic modification is higher by $\nu_e/\omega \approx \nu_e/(C_S/L)$ for $\omega \approx C_S/L$.

7. SUMMARY

In this synopsis we have attempted to present a basis for the physical understanding of drift modes as well as an indication of the background for some of the drift mode inputs to Ref. 3. For $C_S/Lv_i \gg 1$ and $k\rho_i \sim 1$, drift modes can have growth rates of at least $0.06 C_S/L \approx 0.1 v_{Ti}/L$ compared to cE_y/LB for $E \times B$ modes. (We recall ∇n is in the x-direction.) Further drift modes do not require $E \times B \cdot \nabla n > 0$ as do $E \times B$ modes. If one neglects electric field effects in the direction of the density gradient entirely, from Table 1 and Ref. 3, drift modes should be capable of preventing striations from getting thinner than 0.1 km in many cases of interest. The treatment of the condition $E \cdot \nabla n \neq 0$ ($E_x \neq 0$) as it relates to drift modes is an ongoing problem.

REFERENCES

1. L. M. Linson and J. B. Workman, "Formation of Striations in Ionospheric Plasma Clouds," *J. Geophys. Res.* 75, 3211 (1970).
2. P. K. Chaturvedi and P. K. Kaw, "An Interpretation for the Power Spectrum of Spread F Irregularities," *J. Geophys. Res.* 81, 3257 (1976).
3. S. R. Goldman, "Aspects of Striation Decay," JAYCOR Report, (1976).
4. E. Costa and M. C. Kelley, "Calculations of Equatorial Scintillations at VHF and Gigahertz Frequencies Based on a New Model of the Disturbed Equatorial Ionosphere," preprint (1977).
5. S. R. Goldman, "Velocity Shear, The $E \times B$ Instability and the k^{-2} Power Density Spectrum," JAYCOR Report (1976).
6. F. F. Chen, "Introduction to Plasma Physics," Plenum Press, New York (1974).
7. M. K. Hudson and C. F. Kennel, "The Collisional Drift Mode in a Partly-Ionized Plasma," *J. Plasma Phys.* 14, 135 (1976).
8. B. D. Fried and S. D. Conte, "The Plasma Dispersion Function," Academic Press, New York (1961).
9. A. Hasegawa, "Plasma Instabilities in the Magnetosphere," *Rev. Geophys. & Space Phys.* 9, 703 (1971).
10. T. H. Dupree, "Non-linear Theory of Low Frequency Instabilities," *Phys. Fluids* 11, 2680 (1968).
11. J. L. Sperling, private communication (1977).

PART 3

VELOCITY SHEAR, THE $E \times B$ INSTABILITY
AND THE κ^{-2} POWER DENSITY SPECTRUM

PRECEDING PAGE BLANK-NOT FILMED

CONTENTS

	<u>Page</u>
1. INTRODUCTION	3-3
2. GENERAL ANALYSIS	3-6
3. ASYMPTOTIC ANALYSIS FOR $kL E_x/E_y \gg 1$, $kL \gg 1$	3-8
4. ASYMPTOTIC ANALYSIS FOR $kL E_x/E_y \approx 1$, $kL \gg 1$	3-13
5. SUMMARY OF $E \times B$ MODES WITH BACKGROUND PLASMA VELOCITY SHEAR	3-19
6. RELEVANCE TO THE k^{-2} POWER DENSITY SPECTRUM	3-21
REFERENCES	3-25

1. INTRODUCTION

$E \times B$ modes, analogous to the fluid-dynamic Rayleigh-Taylor mode have long been recognized as a significant element for plasma density fluctuation production in the ionosphere.⁽¹⁻⁴⁾ Observations of density fluctuations in the ionosphere indicate some tendency for

$$\left| \frac{n_1(k)}{n} \right|^2 \propto \frac{1}{k^2}$$

where $n_1(k)$ is the amplitude of the one-dimensional density fluctuation at wave-number k and n is the background density.⁽⁵⁻⁷⁾ Numerical simulation which presumably mimics $E \times B$ mode dynamics has also indicated an algebraic variation of the density fluctuation spectrum with k .⁽⁸⁾ A theoretical explanation for the k^{-2} variation based on the decay of $E \times B$ modes into drift modes has recently been presented.⁽⁹⁾ In this work we show that $E \times B$ modes with E_x/E_y non-zero can account directly for a k^{-2} power density spectrum.

We consider a background (zero-order) geometry with spatial variation only in the x -direction ($\perp \vec{B}$). For the F region where $v_{in}/\omega_{ci} \ll 1$ with v_{in} the ion-neutral collision frequency and ω_{ci} the ion cyclotron frequency, the plasma velocity is $\vec{v} = c\vec{E} \times \vec{B}/B^2$ while the current density is $\vec{j}(x) \propto n\vec{E}$. The condition of a stationary background results in $\partial j_x/\partial x = \partial/\partial x(nE_x) = 0$. Hence $n = n(x)$ and non-zero E_x at any x results in non-zero $E_x = E_x(x)$ for all x , which results in $v_y = v_y(x)$ or a velocity shear $\partial v_y/\partial x = cE_x/(BL)$. [We use $L = L(x) \equiv (n^{-1} dn/dx)^{-1}$; i.e., L is the scale length associated with the ambient density gradient.]

In Section 2, the equation for the $E \times B$ instability in the presence of plasma velocity shear, obtained by Perkins and Doles,⁽¹⁰⁾ is analyzed generally for localized modes. In Section 3, with k the wave number of the $E \times B$ mode in the y -direction, and $kL \gg 1$, the equation is analyzed for the parameter ranges

$$(a) \quad E_x/E_y \ll 1, \quad kL E_x/E_y \gg 1 \quad ,$$

and

$$(b) \quad E_x/E_y \gg 1, \quad kL E_x/E_y \gg 1 \quad .$$

In Section 4, again with $kL \gg 1$, the equation is analyzed for the parameter range

$$(c) \quad kL E_x/E_y \sim 1$$

and the reason for the erroneous conclusion of Perkins and Doles,⁽¹⁰⁾ that $E \times B$ modes are stabilized for $kD(E_x/E_y) > 2$, $kL \gg 1$, is shown (D is a parameter taken roughly equal to L). In Section 5, the modal results are summarized. The analysis for range (b) for modes of the form of Eq. (4), q.v., indicates if the ratio E_x/E_y becomes too large (on a scale of unity) that spatially localized $E \times B$ modes no longer exist. Unstable modes are found throughout ranges (a) and (c). In Section 6 the application to determination of the k^{-2} power density spectrum is presented. The eigenmode structure is such that modes in both ranges (a) and (c), with k large on the scale of $E_y/(E_x L)$, have the same dominant variation,

$$\left| \frac{1}{n_1} \frac{dn_1}{dx} \right| \approx \frac{\sqrt{3}}{3} k \propto k \quad .$$

Mode amplitudes tend to be limited by $|dn_1/dx| = |\nabla n_0|$ because if $|dn_1/dx| > |\nabla n_0|$ modes with $k^* \gg k$ will tend to grow more rapidly than (and presumably at the expense of) the mode with

$n_1(k)$. This leads directly to a k^{-2} spectrum. Competition with the process of decay of $E \times B$ modes into drift modes, which can also lead to a k^{-2} spectrum,⁽⁹⁾ is readily assessed.

2. GENERAL ANALYSIS

Our modal analysis is based on the model of Perkins and Doles⁽¹⁰⁾ which, without further approximation, yields their Eq. (14) which has the form

$$\frac{d^2 \chi}{dx^2} + a \chi = 0 \quad (1)$$

Here

$$a = -k^2 \left[1 - \frac{cE_y B^{-1} n'}{n(\gamma - i\omega)} - \frac{1}{2} \frac{\gamma n''}{n(\gamma - i\omega)} + \frac{1}{4} \left(\frac{\gamma n'}{n(\gamma - i\omega)} \right)^2 \right] \quad (2)$$

with $\omega = kcE_x/B$. The perturbations in plasma density n_1 and electrostatic potential ψ_1 have the form

$$n_1 = n_1(x, k) e^{iky + \gamma t}$$

$$\psi_1 = \psi_1(x, k) e^{iky + \gamma t}$$

χ is related to ψ_1 by

$$\psi_1 = [(\gamma - i\omega)/n]^{\frac{1}{2}} \chi \quad ,$$

and the prime denotes d/dx .

We first solve an equation of the form of Eq. (1) under the assumption of localized modes. Expanding around $x = x_0$ one has

$$a = a_0 + a'(x - x_0) + \frac{a''}{2} (x - x_0)^2 + \dots \quad (3)$$

where $a(x_0) = a_0$. On making use of the substitution $x - x_0 = y + s(x_0)$ and seeking modes with a single peak in magnitude, $|\chi| \propto e^{-\eta y^2}$, $\text{Re } \eta > 0$, one readily obtains with c a constant, $s = -a'/a''$ and:

$$\chi = c \exp \left\{ - (a'')^{\frac{1}{2}} \frac{i\sqrt{2}}{4} \left[(x - x_0)^2 + \frac{2a'}{a''} (x - x_0) + \frac{a'^2}{a''^2} \right] \right\}, \quad (4)$$

while for the eigenvalue condition:

$$a_0 - \frac{a'^2}{2a''} - \frac{i\sqrt{2}}{2} (a'')^{\frac{1}{2}} = 0. \quad (5)$$

One expects x to be localized within a range x^* of x_0 such that

$$|x - x_0| \lesssim \frac{2\sqrt{2}}{|\text{Im}(a'')^{\frac{1}{2}}|^{\frac{1}{2}}} \equiv x^* \quad (6a)$$

provided that

$$\text{Im}(a'')^{\frac{1}{2}} < 0 \quad (6b)$$

and

$$\text{Im} \frac{a'}{(a'')^{\frac{1}{2}}} \approx 0. \quad (6c)$$

Condition (6c) can be written more precisely as:

$$|\text{Im}(a'')^{\frac{1}{2}}| x^* \gg \text{Im} \frac{a'}{(a'')^{\frac{1}{2}}}. \quad (6d)$$

An additional check on validity of the solution procedure is provided by:

$$\left| \frac{1}{3} (x - x_0) \frac{d^3 a}{dx^3} (x_0) \right| \ll |a''| \quad (6e)$$

since higher order terms are neglected in Eq. (3).

3. ASYMPTOTIC ANALYSIS FOR $kL E_x/E_y \gg 1$, $kL \gg 1$

We anticipate that modes exist for which $\gamma - i\omega \sim cE_y/BL$ where \sim denotes equality within a numerical factor of size unity. Since $\omega = kcE_x/B$

$$\frac{\omega}{\gamma - i\omega} \sim kL \frac{E_x}{E_y} \gg 1 \quad (7a)$$

and

$$\gamma = i\omega \quad (7b)$$

to lowest order in $(kL E_x/E_y)^{-1}$. On defining

$$\bar{x} = kx \quad (8)$$

and $\bar{x}_0 = kx_0$, Eq. (1) becomes

$$\chi'' + a_1 \chi = 0 \quad (9a)$$

or:

$$\chi'' + \left[a_{10} + a_1'(\bar{x} - \bar{x}_0) + a_1''(\bar{x} - \bar{x}_0)^2/2 \right] \chi = 0 \quad (9b)$$

where $a_{10} = a_1(\bar{x}_0)$, prime now indicates differentiation with respect to \bar{x} , and

$$a_1 = - \left\{ 1 - \frac{cE_y}{BL\omega} \frac{1}{(\gamma/\omega - i)} - \frac{1}{4} \left[\frac{\gamma/\omega}{kL(\gamma/\omega - i)} \right]^2 + \frac{1}{2} \frac{\gamma/\omega}{(\gamma/\omega - i)} \frac{n''}{n} \right\} \quad (10)$$

Since $\omega/(\gamma - i\omega) \gg 1$ on anticipating $n''/n \approx 1/k^2 L^2$ the final term in a_1 can be neglected compared to the third term; further again to lowest order in $(kL E_x/E_y)^{-1}$,

$$\left[\frac{1}{\omega(\gamma/\omega - i)} \right]' = \frac{1}{\omega} \left[\frac{1}{(\gamma/\omega - i)} \right]' \quad (11)$$

Then on defining $\alpha = E_y(x_0)/E_x(x_0)$, $z = [kL(\gamma/\omega - i)]^{-1}$ and using Eq. (8) and

$$\frac{d\omega}{d\bar{x}} = \frac{-\omega}{kL} \quad (12a)$$

so that

$$\frac{dz}{d\bar{x}} = -i z^2 \quad (12b)$$

we obtain

$$a_1 = - (1 - \alpha z + z^2/4) \quad (13a)$$

$$a_1' = -i \alpha z^2 + i z^3/2 \quad (13b)$$

$$a_1'' = -2 \alpha z^3 + 3 z^4/2 \quad (13c)$$

$$a_1''' = 6i \alpha z^4 - 6i z^5 \quad (13d)$$

It is now convenient to divide the analysis into the opposing limits of $\alpha \gg 1$ and $\alpha \ll 1$. We note that it is simultaneously possible to satisfy $kL E_x/E_y \gg 1$ and $\alpha \gg 1$ provided $kL \gg \alpha \gg 1$. The limit $kL E_x/E_y \gg 1$, $\alpha \ll 1$ is satisfied trivially for $kL \gg 1$.

Limit $\alpha \gg 1$

On letting

$$z = \frac{z_0}{\alpha} + \frac{z_1}{\alpha^2} + \dots \quad (14)$$

and substituting Eqs. (13) and (14) into (5) (which applies to a_1 and \bar{x} as well as a and χ) we obtain on collecting terms $\sim \alpha^0$,

$$z_0 = 4/3 \quad (15a)$$

and terms $\sim \alpha^{-1}$,

$$z_1 = (4/3)^{5/2} \alpha/|\alpha| \quad (15b)$$

Since z_1/z_0 is real, z_1 does not introduce any qualitatively different features into the eigenvalue or the eigenmode. The eigenvalue is given to lowest order in α^{-1} by:

$$\gamma = i\omega_0 + \frac{3}{4} \frac{cE_y}{BL}, \quad (16)$$

with $\omega_0 = \omega(x_0)$.

On using Eqs. (15a) and (15b) in (13b)-(13d) one has, to lowest order in α^{-1} ,

$$a_1' = -i\alpha(z_0/\alpha)^2 \quad (17a)$$

$$a_1'' = -2\alpha(z_0/\alpha)^3 \quad (17b)$$

$$a_1''' = 6i\alpha(z_0/\alpha)^4 \quad (17c)$$

Hence using first Eq. (4) (with a_1 in place of a and \bar{x} in place of x) and then Eq. (8), χ can be written,

$$\chi = c_1 \exp \left[-\frac{1}{2} \left(\frac{4}{3}\right)^{3/2} \frac{k^2(x-x_0)^2}{|\alpha|} - \frac{i\sqrt{3}}{3} \frac{\alpha}{|\alpha|} k(x-x_0) \right], \quad (18)$$

with c_1 a constant.

To verify that the modes are consistently localized we note from Eqs. (18) or (17b) and (6a) that one has

$$x^* = \frac{|\alpha|^{1/2}}{k} 2^{1/2} \left(\frac{3}{4}\right)^{3/4}. \quad (19)$$

Hence for $(x-x_0) \sim x^*$, contributions linear in z_1 (i.e., of relative size $|\alpha|^{-1}$ compared to contributions linear in z_0) are of order $\alpha^{-1/2}$ compared to the first term and do not affect the localization provided by the first term. Also within Eq. (6e) we note:

$$\frac{|(1/3)(x-x_0) d^3 a/dx^2|}{|a''|} = \frac{1}{|\alpha|^{1/2}} 2^{1/2} \left(\frac{4}{3}\right)^{1/2}$$

As a further check we note that the localization in χ implies localization in ψ_1 since

$$\frac{x^* \partial/\partial x [(\gamma - i\omega)/n]^{\frac{1}{2}}}{[(\gamma - i\omega)/n]^{\frac{1}{2}}} \approx |\alpha|^{-\frac{1}{2}} .$$

It is perhaps relevant to turbulent diffusion that the location x_0 around which the mode is "centered" is arbitrary and not determined by any subsidiary condition (as is customary in $E \times B$ wave analysis) such as $d/dx(n^{-1} dn/dx)(x_0) = 0$. Hence $E \times B$ instabilities would break out throughout a region of non-zero density gradient of appropriate direction, not merely around the location \bar{x} , although of course growth would be most rapid for x_0 such that $n^{-1} dn/dx$ is a maximum.

Limit $\alpha \ll 1$

Since the localization of the modes in the above case depends on $\alpha \gg 1$ it is interesting to determine whether the localization persists for $\alpha \ll 1$. We find that it does not in general. On expanding

$$z = z_0 + \alpha z_1$$

in Eqs. (13), substituting in Eq. (5) and keeping lowest order terms one obtains $z_0^2 = -12/(6\sqrt{3} + 1)$, i.e., in lowest order α_1'' is positive and $\text{Im}\{(\alpha_1')^{\frac{1}{2}}\} \sim |\alpha|$ at the largest. By virtue of Eq. (6a) this leads to $kx^* \gtrsim |\alpha|^{-\frac{1}{2}}$. Then on using Eqs. (13) in Eq. (9b) one finds that the successive higher order derivative terms in (9b) increase at least as rapidly as $|\alpha|^{-\frac{1}{2}}$ and the localization assumption is inconsistent.

Hence the calculations in the two limits $\alpha \gg 1$ and $\alpha \ll 1$ indicate that localized $E \times B$ instability modes are associated with sufficiently large values of α . This suggests that small values of α stabilize the $E \times B$ instability by causing the

normal modes to be non-local so that regions of unfavorable as well as favorable density gradient (see Figure 1) are sampled by the same mode.

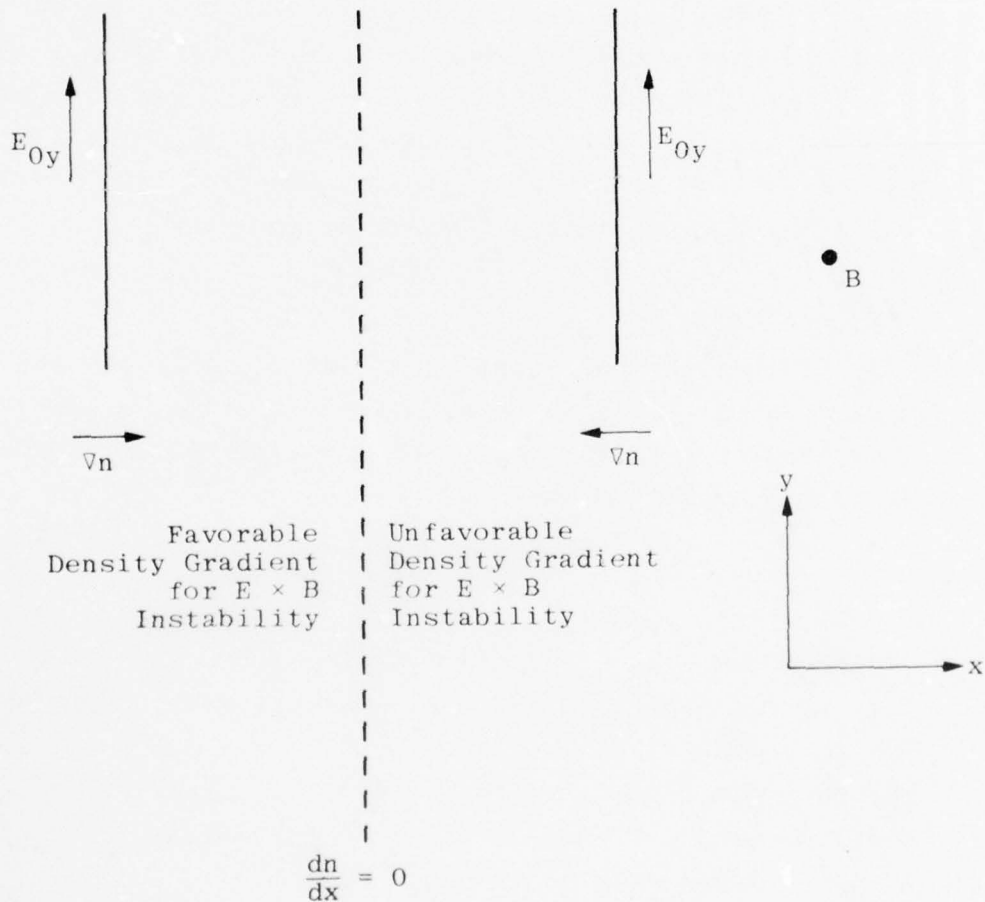


Figure 1. Regions of Favorable and Unfavorable Density Gradient for $E \times B$ Stability.

4. ASYMPTOTIC ANALYSIS FOR $kLE_x/E_y \approx 1$, $kL \gg 1$

For this case we anticipate $z_1(x_0) \equiv \omega_0/(\gamma - i\omega_0) \sim 1$, and define $\beta(x_0) = E_y/(E_x kL)$. Then within Eq. (9b) we have

$$\alpha_1(\bar{x}_0) = - (1 - \alpha_1 z_1) \quad (20a)$$

$$\alpha_1'(\bar{x}_0) = \alpha_2 z_1 - i \alpha_3 z_1^2 \quad (20b)$$

$$\alpha_1''(\bar{x}_0) = \alpha_4 z_1 - i \alpha_5 z_1^2 - \alpha_6 z_1^3 \quad (20c)$$

and

$$\alpha_1 = \beta \quad (21a)$$

$$\alpha_2 = S_2(\bar{x}_0) \beta / (kL) \quad (21b)$$

$$\alpha_3 = \beta / (kL) \quad (21c)$$

$$\alpha_4 = S_3(\bar{x}_0) \beta / (kL)^2 \quad (21d)$$

$$\alpha_5 = [3S_2(\bar{x}_0) - 1] \beta / (kL)^2 \quad (21e)$$

$$\alpha_6 = 2\beta / (kL)^2, \quad (21f)$$

with

$$S_m(\bar{x}_0) = (kL)^m \frac{d}{d\bar{x}^{m-1}} \left(\frac{1}{n} \frac{dn}{d\bar{x}} \right) \quad (22)$$

We expect $S_m(\bar{x}_0) \sim 1$ in general; the possibility $S_m(\bar{x}_0) = 0$ is not excluded.

The expansion for a_1 is clearly valid for modes with spread $\Delta x \ll L$. Since

$$a_1'(\bar{x}_0) \approx (kL)^{-1} \quad (23a)$$

and

$$a_1''(\bar{x}_0) \approx (kL)^{-2} \quad , \quad (23b)$$

from Eqs. (4), (6c) and (6d) one expects that modes should be localized around the region specified by

$$\text{Im} \left[\frac{a_1'}{(a_1'')^{\frac{1}{2}}} \right] = 0 \quad , \quad (6c')$$

with eigenvalues specified by Eq. (5).

From Eqs. (21a) and (21b) we have to order $(kL)^{-1}$ in Eq. (5),

$$a_0 - a'^2/2a'' = 0 \quad . \quad (5')$$

From Eq. (6c')

$$a'^2/a'' > 0 \quad , \quad (6c'')$$

so that $a_0 > 0$; i.e., $\beta z_1 > 1$ or,

$$\frac{cE_y}{BL} \frac{1}{(\gamma - i\omega_0)} > 1 \quad .$$

For $cE_y/(BL) > 0$, this implies $\gamma - i\omega_0 < cE_y/(BL)$. However it also implies $\gamma - i\omega_0 > 0$. Thus the effect of the velocity shear on a localized mode in this region is to lessen the growth rate but not to stabilize the instability, and the question of instability (at least for localized modes in the form of Eq. (4)) becomes equivalent to the existence of localized modes.

With a little algebra we obtain from Eqs. (20) with $H \equiv (\alpha')^2/2\alpha''$, ($H > 0$),

$$H = \frac{z_1}{2} \frac{(2\alpha_2\alpha_3z_1^2 + \alpha_3^2z_1^2 - \alpha_2^2)}{(\alpha_5z_1^2 + \alpha_6z_1^2 - \alpha_4)} \quad (24a)$$

For $\alpha_2 = 0$ or $\alpha_5 = 0$, H cannot be real; hence Eq. (24a) becomes

$$H = z_1 \frac{\alpha_2\alpha_3}{\alpha_5} \frac{[i + (\alpha_3^2z_1^2 - \alpha_2^2)/(2\alpha_2\alpha_3z_1)]}{[i + (\alpha_6z_1^2 - \alpha_4)/(\alpha_5z_1)]} \quad (24b)$$

Positivity (and hence reality) of H results in:

$$z_1^2 \left(\frac{\alpha_3}{2\alpha_2} - \frac{\alpha_6}{\alpha_5} \right) = \frac{\alpha_2}{2\alpha_3} - \frac{\alpha_4}{\alpha_5} \quad (25a)$$

But solving for z_1 requires

$$z_1 = \frac{\alpha_5}{\alpha_1\alpha_5 - \alpha_2\alpha_3} \quad (25b)$$

Eliminating z_1 from Eqs. (25a) and (25b), using Eq. (21) and writing

$$\beta = \frac{E_y}{E_x} \frac{nL}{Lk} \quad ,$$

where n , E_x and L are the respective values of n , E_x , and L at some reference point in x , results in

$$\left(\frac{E_y}{E_x} \frac{nL}{Lk} \right)^2 = - \left(\frac{nL(\bar{x}_0)}{n(\bar{x}_0)L} \right)^2 \frac{(3S_2 - 1)^2 (S_2 + 1)}{(2S_2 - 1)^2 S_2 [S_2(3S_2 - 1) - 2S_3]} \quad (26)$$

with S_2 evaluated at \bar{x}_0 . The value of S_2 is constrained by the condition $\beta z_1 > 0$ which, combined with Eq. (25b), results in

$$1 > \alpha_2 \alpha_3 / (\alpha_1 \alpha_5) > 0 \quad . \quad (26a)$$

This is equivalent to $S_2(\bar{x}_0) < 0$ or $S_2(\bar{x}_0) > 1/2$.

We further note

$$\gamma = i\omega_0 + \frac{cE_y}{BL} \frac{(1 - 2S_2)}{(1 - 3S_2)} \quad . \quad (27)$$

It is clear that at every x_0 with the right-hand side of Eq. (26) positive there is a single "resonant" k . If the right-hand side of Eq. (26) can vary continuously for positive values from 0 to infinity subject to $S_2(\bar{x}_0) < 0$ or $S_2(\bar{x}_0) > 1/2$ then localized unstable modes are in principle possible at all k . Hence the existence of regions in k without localized $E \times B$ modes depends on the form of $n(\bar{x})$ (which determines all other variations on the right-hand side of Eq. (26)).

We now survey the eigenmode behavior for k first large and then small on the scale of $(E_y/E_x L)$.

Large k Limit

Zeroes of the right-hand side of Eq. (26), e.g., $S_2(\bar{x}_0) = -1$, locate accumulation points for modes in the large k limit within the ordering $kL E_x/E_y \sim 1$. We consider several functions $n(x)$ to determine whether such large k modes exist. (For such modes, with $S_2 \approx -1$, $\gamma - i\omega_0 = (3/4) cE_y/(BL)$.)

The functions are:

$$n = n \exp(-x^2/2\tilde{x}^2) \quad , \quad \text{Gaussian} \quad (28a)$$

$$\frac{n'}{n} = \frac{1}{d} \left[1 - \frac{(x - \tilde{x})^2}{D^2} \right] \quad , \quad \text{function used by Perkins and Doles}^{(10)} \text{ in their Eq. (15) with } \tilde{x} \text{ replacing their } x_0 \quad (28b)$$

$$n = n \exp(-\lambda x), \quad \lambda = \text{constant} \quad . \quad (28c)$$

For Eq. (28a), $S_2 = -1$ is attainable at $x = \pm \tilde{x}$ with $x = -\tilde{x}$ corresponding to instability for $E_y > 0$. For Eq. (28b), $S_2 = -1$ is attainable for $x - \tilde{x}$ such that $2d(x - \tilde{x})/D^2 = \{1 - (x - \tilde{x})^2/D^2\}$, i.e., at a value $(x - \tilde{x})/D < 1$. For Eq. (28c), $S_2 = -1$ is not attainable since $S_2 \equiv 0$.

Our results for this limit differ from the results of Perkins and Doles⁽¹⁰⁾ which indicate stability of $E \times B$ modes for $E_x kD/E_y > 2$, i.e., for sufficiently large k within the ordering $E_x kL/E_y \sim 1$. (D is assumed comparable to L .) The analysis of Perkins and Doles⁽¹⁰⁾ is conducted around a point for which $S_2 = 0$; at such a point, appropriate only to the limit $E_x kL/E_y \ll 1$, there is no mode localization for $E_x kL/E_y \geq 1$. One can readily see this from the inconsistency of $(a^*)^2/2a^*$ real and positive, Eq. (24a), and $\alpha_2 = 0$, $\alpha_5 \neq 0$ (from $S_2(\bar{x}_0) = 0$).

Further we note on defining χ_1 to be the "approximate" solution to Eq. (20) of Perkins and Doles⁽¹⁰⁾ (and hence to their Eq. (18), that if one assumes $|\chi_1 - \chi|/\chi \ll 1$ so that $\chi_1 \approx \chi$, one obtains the result

$$I = \left| \frac{d^2(\chi_1 - \chi)}{dx^2} \right| / \left| \frac{d^2\chi}{dx^2} \right| \approx \frac{1}{2} \left(\frac{kLE_x}{E_y} \right)^2 \frac{D^2}{d^2} \frac{cE_y}{BL} \frac{1}{|\gamma - i\omega_0|} \sim 1 \quad , \quad (29)$$

whereas for self consistency one would expect $I \ll 1$. (Here D and d are as defined in Eq. (28b).)

(To see this, we note that in the notation of Perkins and Doles⁽¹⁰⁾ χ_1 satisfies the equation

$$\frac{d^2\chi_1}{d\xi^2} = \left\{ \frac{kD(\gamma^* - 1 + \alpha^2/4) + \xi^2}{\gamma^* + \alpha^2/2} \right\} \chi_1 \quad .$$

On using their Eqs. (17) and (19) with $\gamma_0 = cE_y/Bd$ this becomes

$$\frac{d^2 \chi_1}{dx^2} = k^2 \frac{\left[\gamma - i\omega_0 - \gamma_0 + i\omega_0(x - x_0)/d + \gamma_0(x - x_0)^2/D^2 \right] \chi_1}{\gamma - i\omega_0 + (1/2) \omega_0^2 D^2 / (\gamma_0 d^2)} \quad (30)$$

while their Eq. (18) can be written:

$$\frac{d^2 \chi}{dx^2} = k^2 \frac{\left[\gamma - i\omega_0 - \gamma_0 + i\omega_0(x - x_0)/d + \gamma_0(x - x_0)^2/D^2 \right] \chi}{\gamma - i\omega_0 + i\omega_0(x - x_0)/d} \quad (31)$$

We now replace χ_1 on the right hand side of Eq. (30) by χ and check the consistency of $\chi_1 \approx \chi$ by subtracting Eq. (31) from Eq. (30), thereby obtaining

$$\frac{d^2(\chi_1 - \chi)/dx^2}{d^2\chi/dx^2} = - \frac{\omega_0^2 D^2 / (\gamma_0 d^2) + i\omega_0(x - x_0)/d}{\gamma - i\omega_0 + i\omega_0(x - x_0)/d} \quad (32)$$

On taking $(x - x_0) \sim (D/k)^{\frac{1}{2}}$ and $D \sim d$ we have Eq. (29).)

Small k Limit

Poles of the right hand side of Eq. (26) locate modes with k small on the scale $E_y/(E_x L)$, i.e., $kLE_x/E_y \ll 1$. The value $S_2(\bar{x}_0) = 0$, $d/dx(n^{-1} dn/dx) = 0$, represents the standard no shear ($E_x = 0$) limit with $\gamma - i\omega_0 = cE_y/(BL)$ and $a'/(a')^{\frac{1}{2}} \rightarrow 0$. The value $S_2(\bar{x}_0) = 1/2$ corresponds to zero growth rate. The condition $S_2(3S_2 - 1) - 2S_3 = 0$ appears to present the possibility of additional localized modes, by Eq. (27) not as rapidly growing as those at $S_2 = 0$.

5. SUMMARY OF $E \times B$ MODES WITH BACKGROUND
PLASMA VELOCITY SHEAR

Effects of velocity shear on $E \times B$ modes, i.e., of a non-zero value for E_x , the background electric field in the direction of the background density gradient, depend on the parameter kLE_x/E_y . In all cases we have assumed $kL \gg 1$. One may distinguish three regimes: $kLE_x/E_y \ll 1$, $kLE_x/E_y \sim 1$, and $kLE_x/E_y \gg 1$. For all three regimes if localized modes of the form of Eq. (4) exist they are unstable with growth rate γ_r such that $0 < \gamma_r \leq cE_y/BL$.

The regime $kLE_x/E_y \ll 1$ corresponds to the standard limit in which E_x is neglected. The fastest growing modes (others may possibly exist) are localized around x_0 with $d/dx(n^{-1} dn/dx) = 0$ with $\gamma = cE_y/(BL) + i\omega_0$ and $k_x = |n_1^{-1} dn_1/dx| \approx (k/L)^{1/2} \ll k$.

Modes with $kLE_x/E_y \sim 1$ are determined by Eq. (26) subject to the constraints that the right-hand side of Eq. (26) is positive and either $S_2(x_0) < 0$ or $S_2(x_0) > 1/2$. Corresponding to each value x there is at most a single unstable mode of the form of Eq. (4). Eigenvalues are given by Eq. (27). For this regime it is noteworthy that $k_x = |n_1^{-1} dn_1/dx| \sim k$ whenever the real part of $a'/(a'')^{1/2}$ is non-zero, i.e., whenever $\gamma - i\omega_0 < cE_y/BL$. Attainability of instability at a given k is a function of the ambient density profile. As an example, for k becoming large on the scale of $E_y/(E_x L)$ the values of x_0 approach locations specified by $S_2(x_0) = -1$. Existence of this location is examined in Eqs. (28a)-(28c) for three commonly assumed density profiles. The limit is not attainable for the exponential $n = n \exp(-\lambda x)$ of Eq. (28c) but it exists for a Gaussian and for the function used by Perkins and Doles⁽¹⁰⁾ in their Eq. (15). It is attainable in the vicinity of $d^2n/dx^2 = 0$,

provided $d^3n/dx^3 < 0$ which is generally the case for $dn/dx > 0$; and $d^2n/dx^2 = 0$ is itself attainable whenever the density has a maximum and is constant at its lowest value (at "infinity," for instance). For k becoming small on this scale, $E_y/(E_x L)$, the behavior for the limit $kLE_x/E_y \ll 1$ is approached directly at $S_2 = 0$. In addition "small k " modes appear possible for x_0 satisfying: $S_2(x_0)\{3S_2(x_0) - 1\} - 2S_3(x_0) = 0$. The conclusion of Perkins and Doles⁽¹⁰⁾ that there is stabilization at large k (in this regime) is due to an invalid approximation made after their Eq. (20).

The limit (a), $kLE_x/E_y \gg 1$, and its differentiation from the limit (b), $kLE_x/E_y \sim 1$ but getting large, can best be viewed by separate consideration of the cases $E_y/E_x \gg 1$ and $E_y/E_x \lesssim 1$. For $E_y/E_x \gg 1$, the dominant terms in a_1 and derivatives are the same in both limits; hence the dominant eigenmode-eigenvalue description as given in Eqs. (16) and (18) is the same. From consideration of non-dominant terms in Eqs. (13) and (14), limit (a) is more accurate for $kL > |E_y/E_x|^3$. When it applies, localized modes are indicated over a wide range of x_0 , not just at $S_2(x_0) = -1$ (although it is possible that further analysis would indicate such a tendency for limit (b)). For $E_y/E_x \lesssim 1$, limit (b), which neglects the third term on the right hand side of Eq. (10) and hence contributions $\sim (E_x/E_y)^2$ is inconsistent. However limit (a) with $E_y/E_x \ll 1$ which retains the asymptotically dominant terms for a_1 and derivatives is inconsistent with localized modes of the form of Eq. (4).

These calculations which clearly associate values of E_y/E_x large compared to unity with localized, unstable $E \times B$ modes suggest that values of $E_y/E_x \lesssim 1$ tend to suppress instability by suppressing the existence of localized eigenmodes.

6. RELEVANCE TO THE k^{-2} POWER DENSITY SPECTRUM

Unstable behavior is not seriously inhibited for E_y/E_x large compared to unity and one can generally imagine unstable $E \times B$ modes with very large values of kL , i.e., $kL \gg 1$ while $k\rho_i \ll 1$ with ρ_i the ion Larmor radius. ($\rho_i = c_i/\omega_{ci}$, with c_i the ion thermal speed ($=\sqrt{T_i/m_i}$, with T_i ion temperature and m_i ion mass).) Hence it is reasonable to assume that the parameter range kLE_x/E_y large compared to unity is generally available for unstable $E \times B$ modes. For this range within the limits of either Section 3 or Section 4 the dominant eigenmode structure is the same and is given by Eq. (18), in particular

$$\left| \frac{1}{n_1} \frac{dn_1}{dx} \right| \approx \frac{\sqrt{3}}{3} k$$

If one makes the assumption (as suggested by the work of Sleeper and Weinstock⁽¹¹⁾ when applied to $E \times B$ modes) that modal growth is limited whenever the modal density gradient in the x -direction is comparable in magnitude to the background density gradient

$$|dn_1/dx| \approx n/L \tag{33}$$

one obtains a k^{-2} power density spectrum

$$\left| \frac{n_1(k)}{n} \right|^2 \propto \frac{3}{k^2 L^2} \tag{34}$$

This result is consistent with the L dependence for a k^{-2} power spectrum, $\sim 1/(k^2 L)$, indicated by Ott and Farley.⁽¹²⁾ To see this, on defining m as the running integer variable counting the number of modes, we note that the contribution per unit range in k is given by

$$|n_1(k)|^2 dm/dk$$

analogously to the quantity $\int \Omega(k, \theta) d\theta$ of Ott and Farley. (12)
 If one introduces no new length scales, for a (slight) back-
 ground variation in the y-direction, one has

$$k \propto m\pi/L, \quad m \text{ integral}$$

or

$$dm/dk \propto L$$

from which

$$|n_1(k)|^2 dm/dk = \int \Omega(k, \theta) d\theta \propto (k^2 L)^{-1}.$$

The criterion that modal growth is limited by the condition (33) is reasonable from the standpoint of turbulent cascade considerations, since $|dn_1(k)/dx| \gg n/L$ allows wave numbers $k^* \gg k$ to grow more rapidly than $n_1(k)$, and hence presumably to limit the growth of $n_1(k)$, provided the value of $(E_x + \bar{E}_{x1})/(E_y + \bar{E}_{y1})$ remains small when $|dn_1/dx| \approx n/L$. (Here \bar{E}_{x1} and \bar{E}_{y1} denote the sum over the spectrum in k of the first order electric field components $E_{x1}(k, x) \exp(iky)$ and $E_{y1}(k, x) \exp(iky)$ associated with $n_1(k)$.)

In this connection one notes that the mode density $n_1(k)$ and electrostatic potential, ψ_1 , are connected by Eq. (9) of Perkins and Doles, (10)

$$(\gamma - ik cE_x/B)n_1 = ik \psi_1 (c/B) dn/dx.$$

On taking $\gamma - ikcE_x/B \approx cE_y/BL$ and $k_x = |n_1^{-1} dn_1/dx|$, when $dn_1/dx \approx dn/dx$ this results in

$$ik k_x \psi_1 / E_y = L^{-1}. \quad (35)$$

The contributions to $(\bar{E}_{x1})^2$ and $(\bar{E}_{y1})^2$ are approximately in the ratio $1/3$ for $kLE_x/E_y \gtrsim 1$, but for $kLE_x/E_y \ll 1$ they are in the ratio $k_x/k (\ll 1)$. From Eq. (35) the dominant contributions to $(\bar{E}_{x1})^2$ and $(\bar{E}_{y1})^2$ occur at relatively small kL , which for

sufficiently small E_x/E_y would fall in the range $kLE_x/E_y \ll 1$. Hence provided $E_x/E_y \ll 1$, the ratio $(E_x + \bar{E}_{x1})/(E_y + \bar{E}_{y1})$, which could turn off the instability if it became sufficiently large, tends to remain small at the level of n_1 at which cascade could be driven unless $E_y + \bar{E}_{y1} \rightarrow 0$.

Four additional points may be of interest:

1. Numerical simulation of $E \times B$ instabilities in a plasma slab as summarized in the five cases of Table I of Ref. 10 does not appear to contradict our analysis. Damping for Case 4 ($|E_x/E_y| = 1.8$) is consistent with the breakdown of mode localization for relatively large $|E_x/E_y|$. Faster growth for Case 5 ($k = 4\pi/3$, $|E_x/E_y| = 0.6$) than for Case 3 ($k = 8\pi/3$, $|E_x/E_y| = 0.6$) could be related to the (relatively slight) inhibitory effect of shear with increasing k . (For $kLE_x/E_y \ll 1$ one has cE_y/BL whereas for $kLE_x/E_y \gg 1$ one has $3cE_y/4BL$.) In addition the greater localization and hence difficulty of fully accurate representation of large k modes with a fixed computational mesh spacing could cause more damping at larger k .

2. If one applies the criterion of Eq. (33) to the limit $E_x = 0$ for which $|n_1^{-1} dn_1/dx| \sim (k/L)^{1/2}$, one obtains a k^{-1} spectrum and larger values for $|n_1(k)/n|^2$. A k^{-1} spectrum to our knowledge is not observed. On the other hand, the limit $kLE_x/E_y \gg 1$ would seem in general attainable for E_x/E_y small compared to unity and L sufficiently large.

3. The estimate of Eq. (34) can be compared directly with the estimate of Chaturvedi and Kaw⁽⁹⁾ based on limiting of $E \times B$ mode amplitudes by decay into drift-dissipative modes. Detailed calculations indicate that the threshold for drift-dissipative instability is roughly $kn_1(k)C_i/(nv_i) = 3$, with v_i the effective ion collision frequency given by $v_i = v_{in} + 0.3bv_{ii}$, with v_{in} the ion-neutral collision frequency, v_{ii} the ion-ion

collision frequency, and $b = k^2 C_i^2 / \omega_{ci}^2$. Analogously to Eq. (34) this leads to

$$\left| \frac{n_1(k)}{n} \right|^2 \propto \frac{9}{k^2} \frac{v_i^2}{C_i^2} \quad (36)$$

Comparison of Eqs. (34) and (36) indicates that Eq. (34) dominates whenever $L > (C_i/v_i) \sqrt{3}/3$.

4. At relatively long wavelengths for which $kL \sim 1$, since our calculations are all for the limit $kL \gg 1$, there is no particular indication that the power density spectrum varies as k^{-2} . At relatively short wavelengths for which $k\rho_i \sim 1$ the fluid picture on which the $E \times B$ instability is based becomes a poorer approximation, linear stabilization effects are more significant and the availability of unstable $E \times B$ modes for fixed L at yet larger k to limit the modal density gradient is less likely. Hence, here too, a k^{-2} spectrum is not indicated by our arguments.

To summarize, these calculations indicate that a k^{-2} power density spectrum for k such that $kL \gg 1 \gg k\rho_i$ can be a natural consequence of the eigenmode structure for $E \times B$ modes with $E_x/E_y \neq 0$. The picture is that $E \times B$ modes over a wide range of k are unstable off the primary gradient length $L = (n^{-1} dn/dx)^{-1}$, that they grow until limited by a condition $|dn_1/dx| \propto n/L$, and that this involves a k^{-2} power density spectrum because of the eigenmode structure for $kLE_x/E_y \geq 1$, i.e., $|dn_1/dx| \propto kn_1$. The usage of the criterion $|dn_1/dx| = n/L$ is of course approximate and more detailed study of the non-linear modal behavior should involve a fuller accounting of linear properties, the dynamics of modal interactions, and other possible turbulent (or wave mode dependent) processes.

REFERENCES

1. Linson, L. M. and J. B. Workman, "Formation of Striations in Ionospheric Plasma Clouds," J. Geophys. Res. 75, 3211 (1970).
2. Balsley, B. B., G. Haerendal and R. A. Greenwald, "Equatorial Spread F: Recent Observations and a New Interpretation," J. Geophys. Res. 77, 5625 (1972).
3. Hudson, M. K. and C. F. Kennel, "Linear Theory of Equatorial Spread F," J. Geophys. Res. 80, 4581 (1975).
4. Kelley, M. C., G. Haerendal, H. Kappler, A. Valenzuela, B. B. Balsley, D. A. Carter, W. L. Ecklund, C. W. Carlson, B. Häusler and R. Torbert, "Evidence for a Rayleigh-Taylor Type Instability and Upwelling of Depleted Density Regions During Equatorial Spread F," Geophys. Res. Letts. 3, 448 (1976).
5. Dyson, P. L., J. P. McClure and W. B. Hanson, "In Situ Measurements of the Spectral Characteristic of Ionospheric Irregularities," J. Geophys. Res. 79, 1497 (1974).
6. Costa, E. and M. C. Kelley, "Calculations of Equatorial Scintillations at VHF and Gigahertz Frequencies Based on a New Model of the Disturbed Equatorial Ionosphere," preprint (1977).
7. Crane, R., "Spectra of Ionospheric Scintillation," J. Geophys. Res. 81, 2041 (1976).
8. Scannapieco, A. J., S. L. Ossakow, S. R. Goldman and J. M. Pierre, "Plasma Cloud Late-Time Striation Spectra," J. Geophys. Res. 81, 6037 (1976).
9. Chaturvedi, P. K. and P. K. Kaw, "An Interpretation for the Power Spectrum of Spread-F Irregularities," J. Geophys. Res. 81, 3257 (1976).
10. Perkins, F. W. and J. H. Doles, III, "Velocity Shear and the $E \times B$ Instability," J. Geophys. Res. 80, 211 (1975).

11. Sleeper, A. M. and J. Weinstock, "Nonlinear Theory of Density Fluctuations in Turbulent Plasmas," Phys. Fluids 15, 1507 (1972).
12. Ott, E. and D. T. Farley, "The k Spectrum of Ionospheric Irregularities," J. Geophys. Res. 79, 2469 (1974).

DISTRIBUTION LIST

DEPARTMENT OF DEFENSE

Director
Defense Advanced Research Proj. Agency
ATTN: Strategic Tech. Office

Defense Documentation Center
Cameron Station
12 cy ATTN: TC

Director
Defense Nuclear Agency
ATTN: TISI, Archives
ATTN: DDST
ATTN: RAAF
3 cy ATTN: TITL, Tech. Library

Commander
Field Command
Defense Nuclear Agency
ATTN: FCPR
ATTN: FCPRQ

Director
Interservice Nuclear Weapons School
ATTN: Document Control

Chief
Livermore Division, Field Command, DNA
Lawrence Livermore Laboratory
ATTN: FCPRL

OJCS/J-3
ATTN: WWMCCS, Eval. Ofc., Mr. Toma

Dir. of Defense Research & Engineering
Dept. of Defense
ATTN: S&SS (OS)

Assistant Secretary of Defense
Command, Control, Comm. & Intell.
Dept. of Defense
ATTN: M. Epstein

DEPARTMENT OF THE ARMY

Commander/Director
Atmospheric Sciences Laboratory
US Army Electronics Command
ATTN: DRSEL-BL-SY-S, F. E. Niles

Director
BMD Advanced Tech. Center
Huntsville Office
ATTN: ATC-T, Melvin T. Capps

Commander
Harry Diamond Laboratories
ATTN: DRXDO-NP, Francis N. Wimenitz
ATTN: DRXDO-TI, Mildred H. Weiner
ATTN: DRXDO-NP, Cyrus Mgazed

Director
TRASANA
ATTN: ATAA-SA

DEPARTMENT OF THE ARMY (Continued)

Commander
US Army Electronics Command
ATTN: DRSEL-NL-RD, H. S. Bennet

Commander
US Army Materiel Dev. & Readiness Cmd.
ATTN: DRCLDC, J. A. Bender

Commander
US Army Nuclear Agency
ATTN: MONA-WE, J. Berberet

DEPARTMENT OF THE NAVY

Chief of Naval Research
Navy Department
ATTN: Code 418

Director
Naval Research Laboratory
ATTN: Code 7700, Timothy P. Coffey
ATTN: Code 7750, Jay Boris
ATTN: Code 7750, Joan Pierre
ATTN: Code 7750, Sid Ossakow

Commander
Naval Surface Weapons Center
ATTN: Code WA501, Navy Nuc. Prgms. Off.

DEPARTMENT OF THE AIR FORCE

AF Geophysics Laboratory, AFSC
ATTN: OPR, Harold Gardner
ATTN: OPR, Alva T. Stair
ATTN: SUOL, Research Lib.

AF Weapons Laboratory, AFSC
ATTN: SUL
ATTN: DYT, Maj T. Johnson
ATTN: DYT
ATTN: DYT, Capt L. Wittwer

AFTAC
ATTN: TF/Maj Wiley

SAMSO/SZ
ATTN: SZJ, Major Lawrence Doan

ENERGY RESEARCH & DEVELOPMENT ADMINISTRATION

Los Alamos Scientific Laboratory
ATTN: Doc. Con. for John Zinn

Sandia Laboratories
ATTN: Doc. Con. for W. D. Brown, Org. 1353

OTHER GOVERNMENT AGENCIES

Department of Commerce
Office of Telecommunications
Institute for Telecom Science
ATTN: William F. Utlaut

DEPARTMENT OF DEFENSE CONTRACTORS

ESL, Inc.

ATTN: James Marshall

General Electric Company

Space Division

Valley Forge Space Center

ATTN: M. H. Bortner, Space Sci. Lab.

General Electric Company

TEMPO-Center for Advanced Studies

ATTN: Tim Stephens

ATTN: DASIAC

ATTN: Warren S. Knapp

ATTN: Tom Barrett

ATTN: Mack Stanton

General Research Corporation

ATTN: John Ise, Jr.

Jaycor

ATTN: S. R. Goldman

M.I.T. Lincoln Laboratory

ATTN: Lib. A-082 for David M. Towle

Mission Research Corporation

ATTN: F. Fajen

ATTN: Ralph Kilb

ATTN: Dave Sowle

ATTN: R. Hendrick

ATTN: P. Fischer

ATTN: D. Sappenfield

DEPARTMENT OF DEFENSE CONTRACTORS (Continued)

Physical Dynamics, Inc.

ATTN: Joseph B. Workman

R & D Associates

ATTN: Bryan Gabbard

ATTN: Robert E. LeLevier

Science Applications, Inc.

ATTN: Lewis M. Linson

ATTN: Daniel A. Hamlin

ATTN: D. Sachs

Stanford Research Institute

ATTN: Walter G. Chestnut

ATTN: Charles L. Rino

VisiDyne, Inc.

ATTN: Charles Humphrey

McDonnell Douglas Corporation

ATTN: W. P. Olson